THE JOURNAL OF PHYSICAL CHEMISTRY B

Article

Molecular Dynamics Simulations of a Reversibly Folding #-Heptapeptide in Methanol: Influence of the Treatment of Long-Range Electrostatic Interactions

Maria M. Reif, Vincent Kra#utler, Mika A. Kastenholz, Xavier Daura, and Philippe H. Hu#nenberger

J. Phys. Chem. B, **2009**, 113 (10), 3112-3128• DOI: 10.1021/jp807421a • Publication Date (Web): 19 February 2009

Molecular Dynamics Simulations of a Reversibly Folding β-Heptapeptide in Methanol: Influence of the Treatment of Long-Range Electrostatic Interactions

Maria M. Reif,[†] Vincent Kräutler,[†] Mika A. Kastenholz,[†] Xavier Daura,[‡] and Philippe H. Hünenberger*[,†]

Laboratory of Physical Chemistry, ETH Zürich, CH-8093 Zürich, Switzerland, and Catalan Institution for Research and Advanced Studies (ICREA) and Institute of Biotechnology and Biomedicine (IBB), Universitat Autònoma de Barcelona, E-08193 Bellaterra (Barcelona), Spain

Received: August 19, 2008; Revised Manuscript Received: November 30, 2008

Eight 100-ns molecular dynamics simulations of a β-heptapeptide in methanol at 340 K (within cubic periodic computational boxes of about 6-nm edge) are reported and compared. These simulations were performed with three different charge-state combinations at the peptide termini, one of them with or without a neutralizing chloride counterion, and using either the lattice-sum (LS) or reaction-field (RF) scheme to handle electrostatic interactions. The choice of the electrostatic scheme has essentially no influence on the folding−unfolding equilibrium when the peptide termini are uncharged and only a small influence when the peptide is positively charged at its N-terminus (with or without inclusion of a neutralizing chloride counterion). However, when the peptide is zwitterionic, the LS scheme leads to preferential sampling of the high-dipole folded helical state, whereas the RF scheme leads to preferential sampling of a low-dipole unfolded salt-bridged state. A continuum electrostatics analysis based on the sampled configurations (zwitterionic case) suggests that the LS scheme stabilizes the helical state through artificial periodicity, but that the magnitude of this perturbation is essentially negligible (compared to the thermal energy) for the large box size and relatively polar solvent considered. The results thus provide clear evidence (continuum electrostatics analysis) for the absence of LS artifacts and some indications (still not definitive because of the limited sampling of the folding−unfolding transition) for the presence of RF artifacts in this specific system.

I. Introduction

The treatment of long-range electrostatic interactions in explicit-solvent molecular dynamics (MD) simulations of solvated (bio)-molecules has been a long-standing area of active research.[1−23] Evaluating (and improving) both the accuracy and efficiency of this treatment is essential, because (i) the calculation of electrostatic interactions typically represents the most computationally intensive component of a simulation, (ii) this evaluation always relies on some approximate scheme when attempting to model bulk solution behavior while simulating a truly microscopic solution volume, and (iii) the simulation results can be extremely sensitive to the choice of a specific scheme. In some cases, the latter sensitivity is so important that the application of different electrostatic schemes in otherwise identical simulations leads to qualitatively different conclusions concerning the investigated system.[24,25,27,44,103,104,112,188−190,196,200−203,215,217,234,235,241,247,252] (However, as pointed out in a number of recent studies,[24−27] this could also, in some cases, be related to sampling issues; see below.)

The vast majority of explicit-solvent simulations of solvated (bio)molecules are currently performed under periodic boundary conditions[28−30] (PBC), in order to avoid problems associated with the existence of a liquid−vacuum interface in a (microscopic) system simulated under fixed boundary conditions (FBC; e.g., the need to calibrate appropriate confinement and reaction-field potentials[31−46] that prevent solvent evaporation, correct for the perturbation of the solvent structure at the interface, reintroduce approximate long-range solvation forces, and compensate for surface tension effects and the resulting pressure increase). Under PBC, electrostatic interactions are commonly handled in either of four (approximate) ways: (i) lattice-sum (LS) methods, (ii) straight cutoff (SC) methods, (iii) reaction-field (RF) methods, and (iv) modified truncation (MT) methods.

LS methods[47−54] rely on accepting the periodicity and anisotropy of electrostatic interactions under PBC as an intrinsic property of the simulated system. In this case, electrostatic interactions can be handled exactly (i.e., only within the limit of numerical accuracy) using the Ewald[47] or related lattice-summation,[55−65] particle-mesh [P^{3}M[54,66] or (S)PME],[67,68] fast multipole (FMM[69−84] under PBC), multigrid (MG[85−87] under PBC), fast-Fourier Poisson (FFP[88,89] under PBC), or Maggs[90−94] approaches. This approximation is certainly quite reasonable for the simulation of inherently periodic systems such as crystals. However, solutions are nonperiodic media, and the use of LS methods in this context can be summarized as providing exact electrostatic interactions for an approximate (i.e., artificially periodic) representation of the system.

SC methods[4,29] rely on truncating the electrostatic interactions to a finite (nearest-image) range (cutoff distance), typically less than one-half of the smallest box dimension, and neglecting the contribution of longer-ranged interactions. To reduce the associated error, the truncation is commonly applied on a charge-group basis[4,29] (where charge groups are chosen to be overall neutral atom groups whenever possible). However, given the relatively short cutoff distances that can be used in practice, straight truncation is seldom a justifiable approximation for systems involving atomic charges, because of the long-range

* Corresponding author: Dr. Philippe H. Hünenberger, ETH Zürich, Laboratorium für Physikalische Chemie, ETH−Hönggerberg, HCI, CH-8093 Zürich, Switzerland. Phone: +41 44 632 5503. Fax: + 41 44 632 1039. E-mail: phil@igc.phys.chem.ethz.ch.

[†] ETH Zürich.

[‡] Universitat Autònoma de Barcelona.

10.1021/jp807421a CCC: $40.75
Published on Web 02/19/2009

nature of the Coulomb potential (even in the most favorable case of dipole−dipole interactions between neutral charge groups).

RF methods[95−100] also rely on cutoff truncation. However, the mean effect of the omitted electrostatic interactions beyond the cutoff distance is approximately reintroduced (in a pairwise form) by assuming that the medium outside the cutoff sphere of each particle behaves as a homogeneous dielectric medium of permittivity ϵ_S equal to that of the solvent. This scheme is typically also applied with charge-group cutoff truncation (although atom-based schemes have also sometimes been considered[98,101−104]). The RF approximation is certainly reasonable (given a large enough cutoff distance) for the simulation of pure (dipolar) liquids. However, (bio)molecular solutions are typically dielectrically heterogeneous (i.e., the medium outside the cutoff sphere of a particle is generally not of homogeneous permittivity) and rich in species (solute functional groups, counterions) bearing net charges (i.e., for which the RF formalism is not strictly applicable). Thus, the use of RF methods in this context (in comparison to LS methods) can be summarized as providing approximate electrostatic interactions for a more realistic (i.e., quasi-nonperiodic in terms of long-range electrostatics) representation of the system.

Finally, MT methods rely on cutoff truncation of the electrostatic interactions along with an ad hoc modification of their functional form via switching,[7,105−112] shifting[7,105−108,111−123] or damping[124−127] schemes (both group- and atom-based cutoff truncation have been used in MT schemes[103,104,111,112,128−131]). Note that the SC scheme can be viewed as a special MT scheme with no modification after truncation and that the RF scheme becomes equivalent to the SC scheme in the limit $\epsilon_S \rightarrow 1$ (no solvent) and to an MT (shifting) scheme in the limit $\epsilon_S \rightarrow \infty$ (conducting solvent; almost satisfied in practice for polar solvents).

For completeness, it should be added that a number of approaches have been proposed to alleviate the artificial long-range periodicity and anisotropy induced by the use of LS methods under PBC. Among these, one can mention (i) orientational averaging of the LS potential[113,119,121−123] (effectively leading to a MT scheme), (ii) hybridization of LS with FBC or RF methods,[100,132−136] and (iii) use of hyperspherical boundary conditions[137−147] (HSBC). However, these methods have found only limited use in practical applications (compared to the most popular LS, SC, RF, and MT methods). Note finally that the truncation of van der Waals interactions can also have a significant impact on the properties of simulated systems, such as the energy and the pressure (but much less on the forces). This can be largely remedied by using LS-type schemes[71,100,148−158] or tail corrections[29,150,151,156,159−166] for these interactions.

Irrespective of the selected electrostatic scheme (LS, SC, RF, or MT), simulations of systems under PBC also require the choice of a somewhat elusive parameter: the relative dielectric permittivity ϵ' of the medium surrounding the infinite periodic system (most often discussed in the context of the LS scheme,[100,167−172] see, however, ref 100). For systems that do not exhibit marked surface polarization effects [e.g., (bio)molecules in solution as opposed to crystals], vacuum dielectric boundary conditions[167] ($\epsilon' = 1$) are rarely applied. Although some groups recommend the use of adjusted dielectric boundary conditions[168−171] ($\epsilon' = \epsilon'_S$, where ϵ'_S is the relative dielectric permittivity of the solvent model), in this case, tin-foil dielectric boundary conditions ($\epsilon' = \infty$) are most commonly employed, because they naturally arise from a standard implementation of the different electrostatic schemes (i.e., in the absence of any special correction term related to the dipole moment and, possibly, quadrupole moment[100] of the computational box). Although adjusted dielectric boundary conditions appear to be the most meaningful choice for solutions, they hardly differ from tin-foil dielectric boundary conditions in the case of polar solvents (e.g., water or methanol). In addition, because the correction term enforcing adjusted (or vacuum) dielectric boundary conditions depends on the dipole (and, possibly, quadrupole) moment of the computational box, which is neither continuous in time nor invariant upon translation of the reference computational box (unless the system exclusively consists of neutral groups; see, however, the possible use of corresponding itinerant quantities[173]), the use of tin-foil boundary conditions might actually be preferable.

In view of the expected high impact of the choice of an electrostatic scheme on the simulation results for systems involving atomic charges, a considerable amount of work has been devoted over the past four decades to the problem of assessing the relative accuracies of the different available schemes. An overview of these previous studies is provided in Tables 1 and 2. Taken as a whole, these studies provide fairly clear-cut conclusions for simple systems (Table 1). Recent overviews can be found elsewhere[172] concerning pure (dipolar) liquids;[99,127,130,131,164,170,174] free solvated ions at infinite dilution;[103,170,175−178] solvated ion pairs at infinite dilution;[170,175−178] and ionic crystals, melts, liquids or solutions.[101,117,127,179] However, the results remain surprisingly inconclusive for more complex systems such as solvated biomolecules (Table 2).

The only nearly consensual view (see, however, refs 180–186) is that the SC scheme leads to severe artifacts in various structural and dynamical properties of simulated biomolecular systems,[24,25,27,107,111,112,114,120,187−204] given the relatively short cutoff distances that can be used in practice, just as it does for simpler systems.[95,97−99,104,106,111,114,127,131−133,167,169,170,177−179,205−207,209−232,234−236] However, some (cutoff-based) MT schemes have been suggested to perform well for biomolecular simulations, at least for some systems[107,110,111,114,120,121,129,200,237] and when used in conjunction with sufficiently large cutoff radii. Still, other studies have reported the failure of some of these schemes.[108,112,180,238−241] The same ambiguity holds for the RF scheme. A number of studies have suggested that the RF scheme provides accurate results,[25,27,190,198,200,203,242,244,245] whereas others have pointed toward deficiencies.[199,202,243,246,247] In broad terms, it appears that the RF scheme, initially designed for purely dipolar systems, performs well for systems involving dipole−dipole[95,98,99,174,190,207−210,220,225,248,249] and, to a lesser extent, charge−dipole[97,101,104,169,219,227,230,250] interactions, but could induce significant artifacts in systems rich in species bearing net charges.[101,177,178,202,231,247] Finally, the nature and magnitude of possible periodicity-induced artifacts in biomolecular simulations employing the LS scheme remains a very controversial matter, as various independent studies suggest that they are either significant[54,121,136,203,251−253] or negligible.[24−27,44,112,171,172,186,188,189,191,192,194−196,198−202,204,237,239,241,243−247,320−330,332]

To understand why it is so difficult to draw unambiguous conclusions from these numerous investigations, it is useful to categorize the approaches that have been used to tackle the problem. This can be done as follows (Tables 1 and 2): (A) comparison of the results of simulations performed using different electrostatic schemes under otherwise identical conditions, (B) comparison of the results of a simulation performed using a specific scheme with experimental data or intuition-based expectations, (C) investigation of the sensitivity of the simulation results on the parameters of a specific electrostatic scheme (e.g., scheme variants; box size

TABLE 1: Summary of Previous Investigations Concerning the Influence of the Approximate Electrostatic Scheme and the Possible Presence of Related Artifacts in Simulations of Systems Involving Pure (Dipolar) Liquids; Free Solvated Ions at Infinite Dilution; Solvated Ion Pairs at Infinite Dilution; and Ionic Crystals, Melts, Liquids, or Solutions[a]

ref(s)	approach	conclusion	ref(s)	approach	conclusion
		Liquids			
95, 209	A, B	RF > SC	225	A	LS ≈ RF > SC
114, 205	A, C	MT > SC	98	A, C	LS ≳ RF > SC
207, 210	A, C	RF > SC	130	A, C	LS ≈ MT
139, 290	B, C	HSBC+	229	A, B, C	LS > RF > SC
248	A, C	LS ≈ RF	170	D	LS ≈ MT, LS+
106	C, D	MT > SC	292	A, B, C	LS > RF
33	C	FBC−	131, 235	A, B, C	LS ≳ MT > SC
208	A, B, C	RF ≳ SC	125	A	LS ≈ MT
115, 291	A	LS ≳ MT	293	C, D	LS ≈ MTc > MT
249	A, B	LS ≳ RF	99	A, C	LS ≈ RF > SC
128	B, C	MT+	174	D	LS ≈ RF
218	A, B, C	RF > SC	294	C	LSc ≳ LS
181	A, B	LS > SC > MT	295	A, B	LS > RF
167	A, C	LS ≳ SC	234	A, B, C	LS > SC
220	A	RF > SC	296	B	LS+
135	C	LSc ≈ LS	127	A	LS ≈ MT > RF > SC
168	C	LSc > LS	236	A, C	LS ≳ MT > SC
		Solvated Ions			
211, 214	C	SC−	304	A, C	LSc ≈ SCc
213	C, D	SC−	308, 315	A, C	LSc ≈ FBCc
215	C	SC−, SCc−	309	A, C	LSc ≈ MTc
114	A, C	MT > SC	310	C, D	LSc ≈ SCc ≈ FBCc
297	C	FBC+	311−314	A, C	FBC > LS
133, 221	A, C	FBC > SC	226	C, D	SCc > SC
298	A, B, C	LS ≈ MT	227, 230	C, D	RF > MT > SC
219	A, B, C	LS ≈ RF > MT, SC	169	C, D	LS ≈ RF ≈ MT > SC
299, 307	A	LSc ≈ SCc	171	C, D	LSc ≈ MTc
167	A, C	LS ≳ SC	232	B, C	SC−
254	C, D	SCc+	170	C, D	LS ≈ MT > SC, LSc ≈ MTc
223	A, B, C	LS > SC	178	C, D	RF > SC
118	A	LSc ≈ MTc	177	C, D	LS ≳ RF > SC
224	D	SCc > SC	103, 104	A, C, D	LS ≈ RF > MT > SC; LSc ≈ RFc ≈ MTc ≈ SCc ≈ FBCc
300−302	C	LSc > LS	316	B	LSc+
303−305	A, C	LS > FBC	317	C	LS+
54, 136, 175, 306	C, D	LSc > LS			
		Solvated Ion Pairs			
114	A, C	SC−	228	D	SCc > SC
216	C, D	SC−	231	A	LS > RF > SC
217	B, C	LS > MT ≈ SC	170	C, D	LS ≈ MT > SC
111	A, C	MT > SC	178	C, D	RF > SC
97	A, C	LS > RF > SC	177	C, D	LS > RF > SC
135, 318	C	LSc > LS	145	C	HSBC+
222	A, B, C	LS > SC ≳ MT	233	B	LS+
54, 175	C, D	LS+	136	D	LSc > LS
		Ionic Systems			
319	B, C	LS+	143	A, C	HSBC ≈ LS
206	A, C	LS ≈ MT > SC	117	A, C	LS ≈ MT
106	C, D	MT > SC	179	B	SC−
212	C, D	LS > MT > SC	119, 121−123	A, C	MT > LS
132	A, C	LS > SC	146	B	HSBC+
101	C, D	LS ≳ RF	127	A, C	LS ≈ MT, RF > SC

[a] The approach describes the employed investigation methodology (see Introduction): comparison of MD simulations employing different schemes (A), comparison of MD simulations with experimental data or intuition-based expectations (B), investigation of the sensitivity to the parameters of the electrostatic scheme (C), and analysis of the expected perturbation relative to an ideal (Coulombic, nonperiodic) situation using continuum electrostatics or integral equations (D). The considered schemes are (see Introduction): fixed boundary conditions (FBC); hyperspherical boundary conditions (HSBC); and periodic boundary conditions (PBC) with lattice-sum (LS), straight cutoff (SC), reaction-field (RF), or modified truncation (MT) schemes. The modifier "c" indicates that specific modifications were made to the applied scheme or that specific corrections were applied to the calculated results. The conclusion represents an overall statement (tentatively) summarizing the key findings of the study. It is formed with the following operators: is accurate (+), is inaccurate (−), is more accurate than (>), or gives similar results as (≈). The combined ">" and "≈" operator (≳) is used when a scheme is reported to be more accurate for some properties but to give similar results for others or when a scheme is reported to be more accurate for some parameter combinations but to give similar results for others.

L; cutoff distance R_C in SC, RF, and MT; droplet radius S under FBC), and (D) analysis of the expected perturbation induced by approximate electrostatics within a specific scheme (with reference to the ideal case of a macroscopic,

TABLE 2: Summary of Previous Investigations Concerning the Influence of the Approximate Electrostatic Scheme and the Possible Presence of Related Artifacts in Simulations of Systems Involving Peptides, Proteins, Nucleic Acids, Lipid Membranes, and Other Systems[a]

ref(s)	approach	conclusion	ref(s)	approach	conclusion
		Peptides			
114	A, C	MT > SC	24	A, B	LS > SC
239	A, C	LS > MT	25, 27	A, B	LS ≈ RF > SC
320−323	B	LS+	120	A, B, C	MT > SC
188, 189	A, B, C	LS > SC	186	A, B, C	LS ≈ SC
190	A, B, C	RF > SC	26	A, B, C	LS ≳ SC
54, 251	D	LS−	203	A, B	RF > LS > SC
252	C, D	LS−	44	A	LS > FBC
171	C, D	LSc ≈ MTc	136	D	LSc > LS
199	A	LS ≳ RF ≳ SC	present work	A, D	LS > RF, LS+
		Proteins			
107	A, B, C	MT > SC	240	A, B	MT−
238	B	MT−	129	B, C	MT+
108	A	MT−	251	D	LS−
133	A, C	FBC+	242	B	RF+
110	A, B, C	MT ≳ SC	197	B	SC−
180	A, B	SC > MT	198	A, B	LS ≈ RF > SC
191	A, B, C	LS > SC	246	A	LS ≳ RF
111	A, C	MT > SC	244	A, B	LS ≈ RF
193	A	SC−	237	A, B	LS ≈ MT
324, 326, 328	B	LS+	172	D	LS+
192, 195, 196	A, B	LS > SC	121	A, C	MT > LS
204, 325	A, B	LS ≳ SC	329	C	LS+
327	B, D	LS+			
		Nucleic Acids			
114	A, C	MT > SC	251	D	LS−
187	C	SC−	112	A, C	LS > MT ≳ SC
192	A, B	LS > SC	331	B	FBC+
194	A, B, C	LS > SC	243	A, B	LS ≳ RF
182	B, C	SC+	172	D	LS+
330	B, C	LS+	247	A, B, C	LS > RF
		Lipid Membranes			
253	B	LS−	245	A, C	LS ≈ RF
199	A	LS ≳ RF > SC	329, 332	C	LS+
201	A, B, C	LS > SC	241	A, B, C	LS > MT
200	A, B, C	LS ≈ RF ≈ MT > SC	204	A	LS > SC
202	A, B, C	LS > RF > SC			
		Other Systems			
109	A, C	MT+	135	C	LSc > LS
111	A, C	MT > SC	183−185	A, C	LSc > LS, SC > LS

[a] See footnote of Table 1.

nonperiodic, and Coulombic system) in the simpler context of integral equations or continuum electrostatics.

To appreciate why these different approaches could lead to seemingly contradictory results (especially in the context of complex biomolecular systems), one should recall the main factors affecting the results of these investigations: (1) approximate electrostatics (i.e., the target of the assessment), (2) incomplete sampling (i.e., in incompletely sampled systems, distributions might be biased by kinetic effects and by a dependency on the starting configuration; kinetic effects themselves might hide an implicit dependence on the electrostatic scheme), (3) force-field inaccuracies (i.e., even if an "exact" electrostatic scheme were available and exhaustive sampling were possible, simulation results could still differ from experiment as a result of force-field deficiencies), (4) absence of a reference point for accuracy (i.e., the fact that two electrostatic schemes give different results still provides no hint concerning the accuracies of these two schemes in an absolute sense), and (5) inaccuracies in simplified models (in the context of integral equation or continuum electrostatics approaches).

The outcomes of approaches of types A, B, C, and D (Tables 1 and 2) are influenced by factors of types (1, 2, 4), (1, 2, 3), (1, 2, 4), and (1, 2, 5), respectively. Because none of these approaches is able to characterize solely factor 1, it is not surprising that they could lead to different conclusions. Among the most common possible sources of misinterpretations, one might mention (i) the confusion between thermodynamic (conformational bias) and kinetic (sampling-rate bias) artifacts induced by a specific scheme in the absence of exhaustive sampling (e.g., cutoff-based schemes often involve more algorithmic noise and sample conformational space "faster" than the LS scheme; for this reason, a biomolecule might persist longer in its native state when using the LS scheme, even if this state is intrinsically unstable); (ii) the intuitive assumption that, if either of two compared schemes is obviously biased, the other one is automatically correct (e.g., pair distribution functions are typically affected by artifacts at the cutoff distance in cutoff-based schemes, whereas they are smooth for LS schemes, but the presence of an obvious artifact in the former case does not guarantee the absence of less obvious artifacts in

the latter); (iii) the intuitive assumption that a scheme that better "preserves" the native structure of a biomolecule is automatically superior to one leading to larger fluctuations or distortions (e.g., although it is possible to make a biomolecule rigid around its native structure by applying artificial distance restraints, the resulting model is obviously physically incorrect); and (iv) the intuitive assumption that a scheme leading to agreement with experimental data is automatically superior to one leading to larger discrepancies (because such a comparison simultaneously probes the quality of the force field and might be further biased by incomplete sampling).

In view of the above discussion, the lack of consensus apparent in Table 2 (and, to a lesser extent, Table 1) mainly arises from the facts that (i) many of the quoted conclusions might, in fact, not be supported by the performed investigations because of the entanglement of factors of types 1−5 above; (ii) these conclusions are also affected by the specific implementation variants (e.g., tin-foil, adjusted, or vacuum boundary conditions in LS; handling of the self-energy term in LS; nearest-image or spherical truncation in SC; atom- versus group-based cutoff in SC, RF, and MT; numerous MT variants) and scheme parameters (e.g., L, R_C, S) selected for the considered electrostatic schemes; (iii) these conclusions are also affected by the nature of the investigated system (the magnitude of possible electrostatic artifacts is expected to strongly depend on such factors as the solute charge distribution, the concentration of counterions, the polarity of the solvent, the size of the solute cavity, the size of the computational box, the sampled conformations, the force field employed, and the observables monitored); and (iv) these conclusions are seldom, even for a single study, exempt of some ambiguity (e.g., the results might qualitatively differ depending on the system parameters or observables considered).

One way to assess the nature and magnitude of possible artifacts in the simulated observables caused by the application of an approximate electrostatic scheme relies on the use of continuum electrostatics (approach D) to analyze the corresponding perturbation of the system free energy (relative to the ideal situation of Coulombic interactions within a macroscopic nonperiodic system). This analysis can be applied to single solute configurations or to multiple configurations (e.g., taken along model pathways for conformational transitions or generated through explicit-solvent simulations). It has the advantage of presenting a clear reference point for accuracy (point 4), but could still be affected by sampling errors (point 2) and introduces approximations inherent to a simplified (electrostatic) solvation model (point 5). The continuum electrostatics approach was previously used to investigate periodicity-induced artifacts in LS simulations of solvated spherical ions,[54,104,136,170,171,175,176] ion pairs,[170,175,177] and biomolecules,[136,169,171,172,251,252] as well as electrostatics- and (more limited) periodicity-induced artifacts in RF simulations of solvated spherical ions[103,104,177,178,227,230,254] and ion pairs.[169,177,178] In the context of biomolecular systems, continuum electrostatics studies[172,251,252] have provided strong indications for the presence of periodicity-induced artifacts in specific systems when using the LS scheme (see, however, refs 26 and 171). Yet, they have not been able to provide a complete and unambiguous picture of the problem, because (i) they were applied to solute configurations that did not sample a representative portion of the overall configurational space accessible to the corresponding systems (e.g., simplified model denaturation pathway,[251] onset of denaturation in an explicit-solvent simulation,[172,251,252] or single solute conformations in different box sizes[171]) and (ii) the RF scheme was never investigated by this approach in the context of solvated biomolecules.

A few years ago, we reported an MD study of a zwitterionic polyalanine octapeptide in water using the LS scheme based on cubic computational boxes, that evidenced a strong system-size dependence of the simulated properties over 1-ns simulations[252] (approach C). In the smallest box (2-nm edge), the peptide adopted a rather rigid α-helical conformation. In the medium box (3-nm edge), the α-helical conformation was also preserved, but the peptide flexibility was increased. Only in the largest box (4-nm edge) did the (experimentally expected) peptide denaturation occur (predominantly to conformations characterized by a salt bridge between the peptide termini). Based on a continuum electrostatics analysis of the sampled configurations (approach D), these observations were shown to be compatible with the expected conformational dependence and magnitude of periodicity-induced artifacts in the different boxes.[252]

However, these conclusions were recently challenged by another group based on much longer MD simulations (20 ns), as well as repeats of shorter simulations (10 × 1−2 ns), where the suggested systematic differences were not reproduced.[26] As the authors of this new investigation rightfully pointed out, the uniqueness (no simulation repeats) and limited simulation time scale (1 ns) of the original study[252] prevented the achievement of proper sampling, suggesting that the resulting observations were either coincidential (dependence on the arbitrary initial conditions) or induced by a kinetic bias (difference in unfolding rates) rather than a thermodynamic one (difference in relative stabilities of the folded and unfolded states). In addition, the repeats of short simulations[26] failed to evidence any systematic kinetic bias (i.e., a dependence of the unfolding rate on the box size). Judging from these observations, the authors concluded against the presence of LS artifacts for this system and for the considered box sizes. However, two important points should be kept in mind before accepting this new conclusion. First, the considerably longer time scale (20 ns) of these more recent simulations is still insufficient to achieve reversible folding−unfolding transitions in this system, and the new observations might thus also be coincidental. Second, although the new study convincingly shows the absence of a systematic kinetic bias, it still fails to address the problem of a possible thermodynamic bias in the LS scheme. For these reasons, the observations made in the new study[26] do not formally contradict the results of the previous continuum electrostatics analysis,[252] suggesting the presence of a significant thermodynamic bias (at least for the two smallest box sizes considered).

Of course, it is also legitimate to consider possible flaws of the continuum electrostatics analysis.[26] Continuum electrostatics provides a very approximate description of solvation.[3,5,12,20,21,255−262] It assumes sharp dielectric boundaries between homogeneous dielectric regions (which makes little sense at the microscopic level), neglects both nonpolar effects and microscopic structural effects (e.g., electrostriction, dielectric saturation, radial and orientational structuring of the solvent, and specific hydrogen bonding), and is quite sensitive to the particular choices of the underlying parameters (atomic radii and charges, solute internal relative permittivity). However, there are good reasons to think that it still provides accurate estimates in the context of electrostatic artifacts: (i) The above-mentioned sources of inaccuracies are all short-ranged and should largely cancel out upon evaluating differential electrostatic properties (between a specific scheme and the ideal situation of nonperiodic Coulombic interactions), because this difference is principally encompassed within the long-range component. (ii) This analysis, applied to a new scheme devised as a modification of the LS scheme with

a surface charge on the box walls to mimic a nonperiodic Coulombic situation, gave the expected results (i.e., no difference to the ideal situation of nonperiodic Coulombic interactions) with remarkable accuracy.[136] (iii) A number of tests revealed that this differential analysis (unlike the corresponding absolute numbers) is only weakly sensitive to the employed parameters (atomic radii, definition of the solute−solvent boundary). (iv) This differential analysis provides correction terms capable of essentially erasing any methodology dependence in the calculation of ionic solvation free energies using LS, SC, RF, MT, and FBC schemes.[103,104]

As an attempt to revisit the conclusions of the two above-mentioned studies of LS artifacts[26,252] in the context of appropriately sampled simulations, the present study reports and compares eight 100-ns MD simulations of a β-heptapeptide in methanol at 340 K. The simulations were performed within cubic periodic computational boxes of about 6-nm edge, corresponding to the length of the fully extended peptide plus 2.4 nm. To investigate the effect of the terminal peptide charge states, three different charge state combinations at the peptide termini, one of them with or without a neutralizing chloride counterion, were considered. Finally, to evaluate the possible corresponding electrostatics artifacts that could arise from the use of a RF scheme (instead of the LS scheme), each of the four systems was simulated using either the LS or the RF scheme to handle electrostatic interactions. This system was chosen because previous simulations featured multiple reversible folding−unfolding transitions on the considered time scale and temperature, suggesting the sampling of a representative configurational ensemble.[263,264] The eight simulations are compared in terms of various structural properties (averages and distributions). In addition, possible artifacts due to the use of artificial periodicity in the LS scheme are analyzed in detail using the continuum electrostatics approach based on the configurations sampled during both the LS and RF simulations (zwitterionic peptide only). A similar continuum electrostatics analysis is, in principle, also possible for the RF scheme and will be the scope of a forthcoming study.

II. Computational Details

II.1. Molecular Dynamics Simulation. Eight 100-ns MD simulations of the β-heptapeptide with sequence[263,265] β-HVal-β-HAla-β-HLeu-(*S*, *S*)-β-HAla(αMe)-β-HVal-β-HAla-β-HLeu in methanol were performed with three different charge-state combinations at the two peptide termini, one of them with or without a neutralizing chloride counterion, using either the LS or the RF scheme to handle electrostatic interactions. The simulations were carried out using the GROMOS96 package of programs,[266,267] together with the GROMOS 45A3 united-atom force field[268] and a GROMOS-compatible united-atom methanol model.[269] The equations of motion were integrated using the leapfrog scheme[270] with a time step of 2 fs. All bond lengths, as well as the carbon−hydrogen distance in methanol, were constrained by application of the SHAKE algorithm,[271] with a relative geometric tolerance of 10^{-4}. The systems were simulated under PBC based on cubic computational boxes. Solute and solvent degrees of freedom were independently coupled to a heat bath[272] at 340 K with a relaxation time of 0.1 ps. The box dimensions were isotropically coupled to a pressure bath[272] at 1 atm, with a relaxation time of 0.5 ps and an isothermal compressibility of 2.0×10^{-3} kJ^{-1}·mol·nm^3. The center-of-mass motion was removed every 0.2 ps.

The nonbonded interactions were handled using either the LS or the RF scheme within a twin-range cutoff approach[273] (applied on the basis of distances between charge-group centers[266]), with short- and long-range cutoff radii of 0.8 and 1.4 nm, respectively, and an update frequency of 5 time steps for the short-range pair list and intermediate-range interactions.

The LS scheme relied on application of the particle−particle−particle−mesh (P^3M) method,[54,66] using[274] a real-space cutoff of 0.6 nm (applied on the basis of distances between atoms within the short-range pair list), a spherical-hat charge-shaping function, an assignment function of order 3, a finite-difference interpolation of order 3, a mesh of $64 \times 64 \times 64$ grid points, and tin-foil boundary conditions.

The RF scheme relied on application of a reaction-field (force, energy, and virial) correction[95,97] to short- and intermediate-range interactions, so as to approximately account for the mean effect of electrostatic interactions with the solvent beyond a distance of $R_{RF} = 1.4$ nm (equal to the long-range cutoff radius), using the experimental relative dielectric permittivity $\epsilon_{RF} = 17$ for methanol.[275]

Four different types of systems were considered (each simulated using both the LS and RF schemes), differing by the charge states of the N- and C-termini and the possible presence of a neutralizing chloride counterion: uncharged termini (unc); zwitterionic (zwi); and singly charged (positive charge) at the N-terminus, either without (sc+) or with (scn) a single chloride counterion. The autoionization constant of pure methanol[276] (pK_m value of 16.70 at 298 K) and the ionization constants of model compounds representative for the β-peptide termini (e.g., propanoic acid and ethylamine in methanol,[277] with pK_a values of 9.71 and 11.0, respectively, at 298 K), suggest that the scn system best accounts for the experimental situation at neutral pH (i.e., pH 8.35 in methanol).

The starting configurations for each of the four system types were obtained by placing the solute in an extended (all-trans) conformation into a cubic computational box filled by approximately 3000 methanol molecules, allowing for a minimum solute-to-wall distance of 1.2 nm. For the simulations involving a counterion (scn), one randomly chosen methanol molecule was replaced by a chloride ion. From this point onward, the eight simulations were carried out in parallel. In each case, the system was relaxed using steepest-descent energy minimization,[266] followed by three successive MD simulation periods of 2 ps at 40, 150, and 300 K, respectively. The eight production simulations were initiated from this point and carried out for 100 ns with trajectory frames written to file every 0.5 ps for later analysis. A summary of the simulated systems and simulation conditions is provided in Table 3.

TABLE 3: Summary of the Simulated Systems and Simulation Conditions[a]

system	q_N (e)	q_C (e)	N_{Cl}	N_s	N_{MeOH}	L_{sim} (nm)
unc	0	0	0	63	3052	5.91
zwi	1	1	0	63	2966	5.86
sc+	1	0	0	64	3062	5.94
scn	1	0	1	65	3061	5.93

[a] The systems differ in the charge states of the peptide termini (q_N and q_C for the N- and C-terminus, respectively) and the possible presence of a chloride counterion (N_{Cl}): uncharged termini (unc); zwitterionic (zwi); singly-charged N-terminus, no counterion (sc+); singly-charged N-terminus, one neutralizing chloride counterion (scn). The number of solute atoms (N_s), the number of solvent (methanol) molecules (N_{MeOH}), and the (cubic) box edge length (L_{sim}) after equilibration are also indicated. Each of the four systems was simulated at 340 K and 1 atm for a duration of 100 ns using either the LS or RF scheme to handle electrostatic interactions (eight simulations in total).

II.2. Trajectory Analysis. The eight trajectories were analyzed in terms of backbone atom-positional root-mean-square deviation from a model helical structure (RMSD), end-to-end distance (D_{EE}), N-terminal ammonium-to-chloride distance (D_{NC}; simulation scn only), and solute dipole-moment magnitude (M). In addition, for the two zwi simulations, the periodicity-induced perturbation of the electrostatic free energy ($\Delta\Delta G_{el}^{LS}$) was evaluated from a continuum electrostatics analysis of the sampled configurations.

The RMSD was calculated for all backbone (C, C_α, N) atoms with reference to a nuclear-magnetic-resonance (NMR) derived from model helical structure[263,265] (representative of the peptide folded state), using trajectory frames sampled at 10-ps intervals. The end-to-end distance, D_{EE}, was defined as the (nearest-image) distance between the nitrogen atom of the first residue and the carboxyl carbon atom of the last residue and was monitored analogously. The ammonium-to-chloride distance, D_{NC}, was defined as the (nearest-image) distance between the nitrogen atom of the first residue and the chloride counterion (simulation scn only) and was monitored analogously. Finally, the solute dipole-moment magnitude, M, was defined as the norm of the charge-weighted sum of all peptide atom coordinates relative to the peptide center-of-charge taken as the origin (after reconstruction of the covalent connectivity of the molecule by appropriate lattice translations of its constituting atoms) and was monitored analogously. Note that this quantity is origin-dependent only for the sc+ and scn simulations involving a net peptide charge.

The periodicity-induced perturbation of the electrostatic free energy ($\Delta\Delta G_{el}^{LS}$) was estimated (simulation zwi only) based on a continuum electrostatics scheme as described previously,[54,172,175,251,252] using trajectory frames sampled at 100-ps intervals along the two (LS and RF) simulations. For the LS simulation, this quantity represents an estimate for the sampling bias induced by artificial periodicity in the actual simulation. Analysis of $\Delta\Delta G_{el}^{LS}$ for the RF simulation is somewhat artificial and was performed to increase the extent of conformational space considered for the analysis beyond the sole configurations sampled in the LS simulation.

The quantity $\Delta\Delta G_{el}^{LS}$ represents the change in the electrostatic free energy, ΔG_{el}, of the solute−solvent system (reversible charging of the solute, for a given solute configuration) when going from the ideal (ID) situation of a macroscopic nonperiodic system with exact Coulombic interactions to the LS situation of a microscopic periodic system (of size determined by that of the computational box during the simulation) with Ewald-type interactions, i.e.

$$\Delta\Delta G_{el}^{LS} = \Delta G_{el}^{LS} - G_{el}^{ID} \tag{1}$$

This perturbation of the electrostatic free energy can be partitioned (for the given solute configuration) as

$$\begin{aligned}\Delta\Delta G_{el}^{LS} &= \Delta E_{dir}^{LS} + \Delta\Delta G_{slv}^{LS} \\ &= (E_{dir}^{LS} + \Delta G_{slf}^{LS}) - E_{dir}^{ID} + \Delta G_{slv}^{LS} - \Delta G_{slv}^{ID}\end{aligned} \tag{2}$$

where E_{dir}^{ID} and E_{dir}^{LS} account for the direct pairwise electrostatic interaction energies between the solute atoms in the ID and LS situations, respectively; ΔG_{slf}^{LS} accounts for the self-interaction of solute charges in the LS situation (there is no such term in the ideal nonperiodic Coulombic situation); and ΔG_{slv}^{ID} and ΔG_{slv}^{LS} account for the corresponding electrostatic solvation free energies. The computation of the solvation free energies relied on the application of a continuum electrostatics approximation (modeling the solvent as a homogeneous dielectric medium of relative permittivity ϵ_S). All of the above quantities were assumed to correspond to tin-foil boundary conditions (zero potential and normal field) at infinite distance from the solute (nonperiodic case) or at the surface of the infinite periodic system (periodic case).

For simplicity, the terms corresponding to the LS situation (E_{dir}^{LS}, ΔG_{slf}^{LS}, and ΔG_{slv}^{LS}) were calculated assuming a cubic box with a constant edge length of $L = 6$ nm (a value very close to the average box edge over the explicit-solvent simulations; Table 3). To calculate the terms corresponding to the ID situation (E_{dir}^{ID}, ΔG_{slv}^{ID}) based on trajectory frames issued from the explicit-solvent simulations under PBC, the covalent connectivity of the solute molecule was first restored by appropriate lattice translations of its constituting atoms (using the box parameters of the explicit-solvent simulation). This permitted the evaluation of E_{dir}^{ID}. For the computation of ΔG_{slv}^{ID} using continuum electrostatics, the molecule was further centered in a cubic box of edge $L =$ 6 nm (based on its maximum extent along the three Cartesian dimensions), but not rotated. Although not necessary in principle, the same procedure was applied prior to the calculation of the corresponding terms in the LS situation (E_{dir}^{LS}, ΔG_{slv}^{LS}). This was done because (i) E_{dir}^{LS} and ΔG_{slv}^{LS} were calculated using the constant value of $L = 6$ nm for the box edge rather than the real box edge values along the simulations and (ii) the calculation of ΔG_{slv}^{LS} using continuum electrostatics with identical solute positioning and grid parameters as for ΔG_{slv}^{ID} was expected to improve the numerical accuracy of the difference through cancelation of grid discretization errors.

The calculation of E_{dir}^{ID} (for successive trajectory frames) involved a direct Coulomb sum over all solute atom pairs (after reconstruction of the covalent connectivity of the molecule), i.e.

$$E_{dir}^{ID} = \frac{1}{4\pi\epsilon_o}\sum_{i,j>i}\frac{q_i q_i}{r_{ij}} \tag{3}$$

where i and j are solute atoms with charges q_i and q_j, respectively, separated by a distance r_{ij}, and ϵ_o is the permittivity of a vacuum.

The calculation of E_{dir}^{LS} (for successive trajectory frames) relied on a separate LS (Ewald) calculation for the solute atoms, i.e.

$$E_{dir}^{LS} = E_\gamma + E_\eta + E_A \tag{4}$$

where E_γ, E_η, and E_A represent contributions from the reciprocal-space, real-space, and correction terms, respectively. The definition of these three contributions is provided in detail elsewhere[100] (eqs 27−29 therein). Here, a normalized spherical Gaussian charge-shaping function $\gamma(a^{-1}r) = \pi^{-3/2}e^{-a^{-2}r^2}$ (of width $a = 0.17$ nm, applied using a real-space cutoff of $R_{LS} = 0.6$ nm) was used, for which the terms in eq 4 become (for a cubic box of edge L)

$$E_\gamma = (2\epsilon_o L^3)^{-1}\sum_{\mathbf{l}\in\mathbb{Z}^3,\mathbf{l}\neq 0} k^{-2}e^{-a^2k^2/4}\left\{\left[\sum_i q_i\cos(\mathbf{k}\cdot\mathbf{r}_i)\right]^2 + \left[\sum_i q_i\sin(\mathbf{k}\cdot\mathbf{r}_i)\right]^2\right\} \tag{5}$$

$$E_\eta = (4\pi\epsilon_o)^{-1}\sum_i \sum_{j>i} q_i q_j \bar{r}_{ij}^{-1}\mathrm{erfc}(a^{-1}\bar{r}_{ij}^{-1}) \quad (6)$$

and

$$E_A = (8\pi\epsilon_o)^{-1}[-\pi L^{-3}a^2\Big(\sum_i q_i\Big)^2 - (2\pi^{-1/2}a^{-1} + \xi_{LS}L^{-1})\sum_i q_i^2] \quad (7)$$

where $\mathbf{k} = 2\pi L^{-1}\mathbf{l}$, $\mathbf{l}$ being a vector with integer components; $\bar{r}_{ij}$ denotes the nearest-image distance between atoms i and j; erfc is the complementary error function; and $\xi_{LS} \approx -2.837297$. Equations 5−7 have been simplified relative to their more general forms[100] in that (i) the approximation $\gamma(a^{-1}r) < 10^{-6} \approx 0$ for $r \geq R_{LS}$ was used and (ii) no exclusions were taken into account because their contributions to E_{dir}^{ID} and E_{dir}^{LS} cancel out.

The calculation of the (configuration-independent) LS self-term,[54,100,118,278−280] ΔG_{slf}^{LS}, was performed as described elsewhere[100] (eq 30 therein), which becomes (for a cubic box of edge L)

$$\Delta G_{slf}^{LS} = (8\pi\epsilon_o)^{-1}\xi_{LS}L^{-1}\sum_i q_i^2 \quad (8)$$

For the zwitterionic peptide, eq 8 results in $\Delta G_{slf}^{LS} = -123.85$ kJ·mol^{-1}.

The quantities ΔG_{slv}^{ID} and ΔG_{slv}^{LS} were evaluated (for successive trajectory frames) by application of a nonperiodic finite-difference (FD) solver for the Poisson equation[175,281,282] and of a corresponding periodic FD solver,[175] respectively. All continuum electrostatics calculations relied on a cubic computational volume of edge $L = 6$ nm. This choice was compulsory for the periodic calculations (because it approximately matches the box edge length used in the simulations), but was also adopted for mere convenience for the nonperiodic ones. In the latter case, the computational volume should be just large enough that the computed ΔG_{slv}^{ID} value no longer significantly depends on this parameter, which was verified numerically (data not shown). The choice of a common computational volume is also advantageous because it maximizes the cancelation of grid discretization errors between periodic and nonperiodic FD calculations employing identical numbers of grid points along each direction. The FD solver determined the solution of the Poisson equation via a preconditioned Cholesky conjugate-gradient algorithm (similar to that used, e.g., in the program UHBD[281,282]) under either nonperiodic[175,281,282] or periodic[175] boundary conditions. In both cases, the solvation free energy was computed as the difference in electrostatic free-energy between a system where the relative permittivity outside the solute was set to the solvent permittivity ϵ_S or to 1 (two separate calculations). The relative permittivity inside the solute was always set to 1 (nonpolarizable solute), as appropriate for mimicking explicit-solvent simulations excluding an electronic polarization term for the solute atoms. The value of ϵ_S was set to 15, as determined for the methanol model[269] used in the explicit-solvent simulations. The latter value was calculated from two independent 10-ns simulations of 512 methanol molecules in cubic boxes, employing either the LS or the RF scheme (resulting in values of 15.4 and 15.1, respectively, upon application of the appropriate fluctuation formulas[98,210,248,283]). The value $\epsilon_S = 15$ differs slightly from the value ϵ_{RF} used in the RF correction term of the RF simulations, but this discrepancy is expected to have an entirely negligible influence on the results. For all continuum electrostatics calculations, the number of grid points along each direction was set to 100, and the relative convergence criterion for the electrostatic free energy was set to 10^{-6} kJ·mol^{-1}. The atomic radii were based (as previously described[176]) on contact distances between the different solute atoms and the oxygen atom of a simple-point-charges (SPC) water molecule[284] using the Lennard-Jones parameters of the GROMOS 45A3 force field.[268] However, a correction of 0.03 nm was added to these values, corresponding to the difference between a probe radius of 0.17 nm estimated for methanol and the probe radius of 0.14 nm commonly used for water.[285] The polar hydrogen atoms were treated differently and assigned a common atomic radius of 0.08 nm. A systematic increase or decrease of all atomic radii by up to 0.1 nm was found to have no significant impact on the calculated $\Delta\Delta G_{el}^{LS}$ values (data not shown). A variation of the ϵ_S value in the range 10−50 was also found to have no significant influence on the calculated $\Delta\Delta G_{el}^{LS}$ values (data not shown). Only with relative permittivities smaller than about 10 did the magnitude of the solvation contribution to $\Delta\Delta G_{el}^{LS}$ show a noticeable decrease.

The contributions ΔE_{dir}^{LS} and $\Delta\Delta G_{el}^{LS}$ in eq 2 are expected to be strongly anticorrelated[172,175,251,252] (when considering different solute configurations). This is the case because, in the limit of small (nonpolarizable) solute cavities, one expects a relationship of the form

$$\Delta\Delta G_{slv}^{LS} \approx (\epsilon_s^{-1} - 1)\Delta E_{dir}^{LS} \quad (9)$$

which, using eq 2, implies

$$\Delta\Delta G_{el}^{LS} \approx \epsilon_s^{-1}\Delta E_{dir}^{LS} \quad (10)$$

Note that, for the above relationships to hold, it is essential to include the self-term, ΔG_{slf}^{LS}, in ΔE_{dir}^{LS} (eqs 2 and 8). In this case, eqs 9 and 10 become exact in the limit of infinitesimal cavities (i.e., bare charges embedded in a homogeneous dielectric continuum of permittivity ϵ_S).

All of the above analyses were implemented in Java and Jython as extensions to the esra molecular mechanics analysis package.[286] Visualizations were performed using the PyMol[287] program.

III. Results and Discussion

The backbone atom-positional root-mean-square deviation (RMSD) from an NMR-derived model helical structure representative of the peptide folded state[263,265] is shown in Figure 1 as a function of time for the eight simulations (Table 3), together with the corresponding distributions over the entire trajectory.

Visual inspection and hydrogen-bond analysis (data not shown) suggest that the peptide can be considered to be folded when the RMSD value is below about 0.2 nm.[263] According to this criterion, all trajectories exhibit the reversible formation of a helical structure in 2−10 discrete folding events. However, the relative population of the folded state and the average residence time in this state depend largely on the protonation states chosen for the peptide termini (and the possible presence of a neutralizing counterion), as well as on the electrostatic scheme employed during the simulation. The relative folded-state populations (based on an RMSD cutoff of 0.2 nm) for the

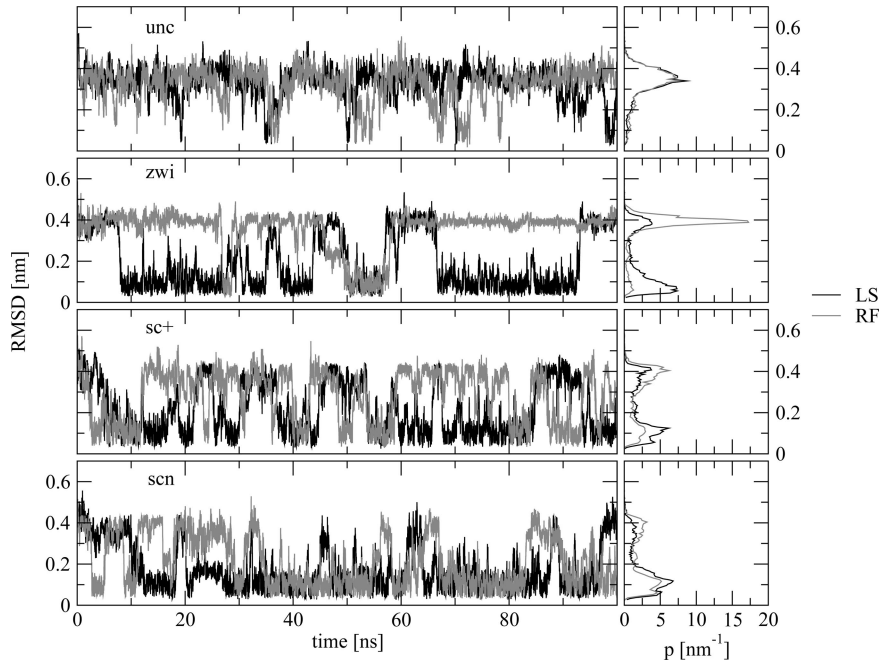

Figure 1. Time evolution and normalized probability distribution (p) of the backbone atom-positional root-mean-square deviation from a model helical structure representative of the peptide folded state[263,265] (RMSD). Simulations using LS and RF electrostatics are shown in black and gray, respectively. From top to bottom (Table 3): uncharged termini (unc); zwitterionic (zwi); singly charged N-terminus, no counterion (sc+); singly charged N-terminus, one neutralizing chloride counterion (scn).

LS simulations are 7%, 63%, 54%, and 71% for the unc, zwi, sc+, and scn systems, respectively, and the corresponding populations for the RF simulations are 11%, 10%, 31%, and 53%, respectively. The residence times in the folded state are on the order of 1 ns for the unc simulations, whereas they are significantly longer in all other simulations. These observations can, in part, be explained (irrespective of the electrostatic scheme employed) in terms of the stabilizing interaction between terminal charges and the backbone dipole associated with a helical conformation.[265] Similar effects of the terminal charge states on the preferential conformations of β-peptides have been reported previously.[265,288,289]

Considering the RMSD distributions, the choice of a specific electrostatic scheme appears to have little or no influence for the systems unc and, to a lesser extent, scn. The difference is much more pronounced for the systems zwi and, to a lesser extent, sc+. In the two latter cases, the LS trajectory predominantly samples the helical conformation, whereas the RF trajectory predominantly samples unfolded conformations.

The end-to-end distance (D_{EE}) is displayed in Figure 2 as a function of time for the eight simulations (Table 3), together with the corresponding distributions over the entire trajectory.

In the unc simulations (for both RF and LS electrostatics), the time evolutions of D_{EE} display rapid (subnanosecond) and high-amplitude fluctuations around a mean value of 1.30 nm. This observation is compatible with the fast sampling of many different (predominantly unfolded; Figure 1) configurations. The corresponding time evolutions in the sc+ and scn simulations (which show similar features here, irrespective of the electrostatic scheme) display equally rapid but lower-amplitude fluctuations around a mean value of about 1.05 nm, interrupted by sporadic excursions toward larger values (residence times of about 5−10 ns). Although a value of 1.05 nm is appropriate for the helical state, comparison with Figure 1 shows that only a fraction of these configurations are actually folded. Thus, in contrast to the unc simulations, only a small subset of the sampled unfolded configurations (RMSD > 0.2 nm) are associated with high end-to-end distances ($D_{EE} \gg 1.05$ nm) in the sc+ and scn simulations. The dominance of less extended configurations (with D_{EE} values close to that of the helical conformation) in the unfolded-state ensemble and the higher folded-state population in the two systems involving a charged N-terminus (compared with the uncharged form) are probably due to favorable interactions between the backbone peptide dipole in moderately extended configurations (or the overall helix dipole in the folded helical state) and the N-terminal charge.[265,288,289]

In the zwi simulations (for both RF and LS electrostatics), the time evolutions of D_{EE} display long-time-scale hopping between two distances, one corresponding to the folded helical state ($D_{EE} \approx 1.05$ nm) and the other corresponding to a set of configurations presenting a salt bridge between the peptide termini ($D_{EE} \approx 0.35$ nm). Illustrative structures for these two states are presented in Figure 3. A strong anticorrelation is also observed here between the time evolutions of the RMSD (Figure 1) and of D_{EE} (Figure 2). The particular stability of the helical and salt-bridged conformations in the context of a zwitterionic peptide can probably be traced back to the large-magnitude and long-range nature of charge−charge interactions, even in a relatively polar solvent such as methanol. The salt-bridged configurations are obviously stabilized by direct ion-pairing interactions. The folded helical state benefits from stabilization through hydrogen bonding and hydrophobic packing, as well as through favorable interactions between backbone dipole and terminal charges, along with a still relatively short end-to-end distance (compared to most of the unfolded structures sampled in the unc and, to a lesser extent, sc+ and scn simulations). Note also the transient formation of highly extended (quasi-linear) structures immediately before and after one of the main transitions to the salt-bridged state in the LS simulation (about 60−66 ns). These conformations might be stabilized through (artificial) interactions between the termini of the peptide in the reference box and the opposite termini of its periodic copies in

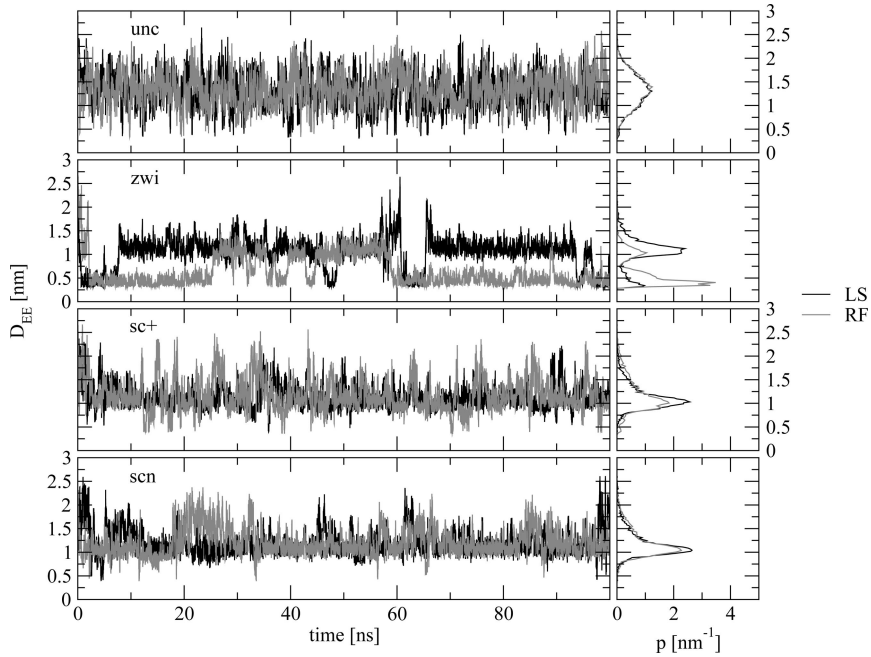

Figure 2. Time evolution and normalized probability distribution (p) of the (nearest-image) end-to-end distance (D_{EE}). Simulations using LS and RF electrostatics are shown in black and gray, respectively. From top to bottom (Table 3): uncharged termini (unc); zwitterionic (zwi); singly charged N-terminus, no counterion (sc+); singly charged N-terminus, one neutralizing chloride counterion (scn). Note that the D_{EE} values are always smaller than the radius of the largest sphere that can be inscribed within the computational box (i.e., about 3 nm).

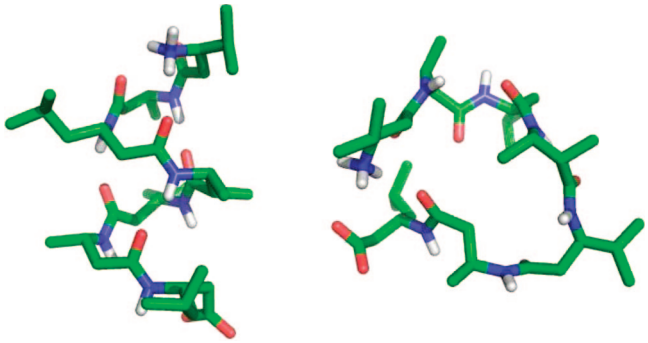

Figure 3. Two representative structures from the simulation of the zwitterionic peptide (zwi; Table 3) with LS electrostatics. Left: trajectory frame sampled at 15 ns, corresponding to the folded helical structure (RMSD = 0.07 nm, D_{EE} = 1.05 nm, and M = 0.70 e·nm). Right: trajectory frame sampled at 65 ns, corresponding to an unfolded salt-bridged configuration (RMSD = 0.36 nm, D_{EE} = 0.40 nm, and M = 0.35 e·nm).

the two neighboring boxes along the direction of its end-to-end axis (see below).

Except for the zwitterionic case, the D_{EE} distributions are essentially insensitive to the electrostatic scheme employed in the simulation. In the unc case, the distributions present a Gaussian shape centered at 1.30 nm and approximately extending from 0.50 to 2.25 nm (full width at half-height of 0.80 nm). In the sc+ and scn cases, a narrow peak is found at about 1.05 nm (folded helical structure, as well as moderately extended unfolded structures), with a sharp lower bound (at about 0.80 nm) and a broader upper tail extending to 2.25 nm. In the zwitterionic case, both LS and RF simulations present two narrow peaks, centered at 1.05 (folded helical state) and 0.35 (salt-bridged configurations) nm, but with different populations as was the case for the RMSD (Figure 1). The LS simulation preferentially samples the more extended helical state, whereas the RF simulation predominantly visits the more compact salt-bridged configurations. Note, however, that the configurations with D_{EE} > 0.75 nm also encompass about 20% unfolded configurations (RMSD > 0.2 nm) in both simulations.

The ammonium-chloride distance (D_{NC}) is shown in Figure 4 as a function of time for the two scn simulations (Table 3), together with the corresponding distributions over the entire trajectory. Both simulations are characterized by multiple pairing events lasting for up to 5 ns, separated by intervals of similar durations. The corresponding distributions (for both LS and RF electrostatics) exhibit a sharp peak at 0.32 nm (contact distance), followed by a well-resolved miminum at 0.6 nm. Beyond this distance, the LS and RF distributions differ. For the LS simulation, the probability increases monotonically with distance up to about 3.0 nm (the distance from the box center to the nearest box walls, above which the probability distribution is distorted by the restriction of the statistics to nearest-image distances). In the RF simulation, however, the distribution is characterized by a relatively sharp peak at about 1.0 nm followed by a broad minimum centered around 2.1 nm, before increasing again to about 3.0 nm.

The peptide dipole-moment magnitude (M) is displayed in Figure 5 as a function of time for the eight simulations (Table 3), together with the corresponding distributions over the entire trajectory.

In simulation unc (for both LS and RF electrostatics), the time evolution of M displays rapid (subnanosecond) fluctuations in the range 0.0−0.5 e·nm. Such low values are expected for a purely dipolar peptide involving no net charges at its termini. The corresponding time evolutions for simulations sc+ and scn (which show similar features here, irrespective of the electrostatic scheme) display equally rapid fluctuations in a similar range, interrupted by sporadic excursions toward larger values (up to 1.3 e·nm with residence times of 1−10 ns), corresponding to nonhelical conformations. However, as observed previously for the end-to-end distance (Figure 2), comparison with Figure 1 suggests that only a small subset of the sampled unfolded configurations (RMSD > 0.2 nm) is characterized by a high

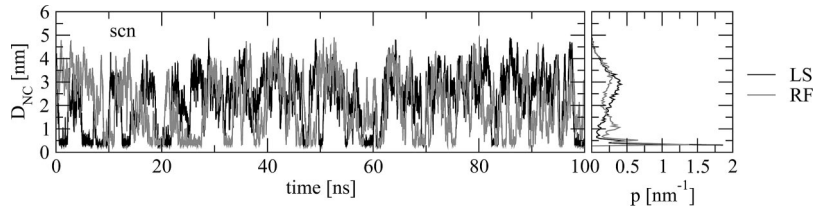

Figure 4. Time evolution and normalized probability distribution (p) of the (nearest-image) distance between the N-terminal ammonium nitrogen atom and the chloride ion (D_{NC}) in the simulation with a charged N-terminus and one neutralizing chloride counterion (scn; Table 3). The simulations using LS and RF electrostatics are shown in black and gray, respectively. Note that the probability distributions might be distorted in the approximate range 3.0−5.2 nm (i.e., the distance from the center of the computational box to the nearest box walls and corners) and become zero above 5.2 nm.

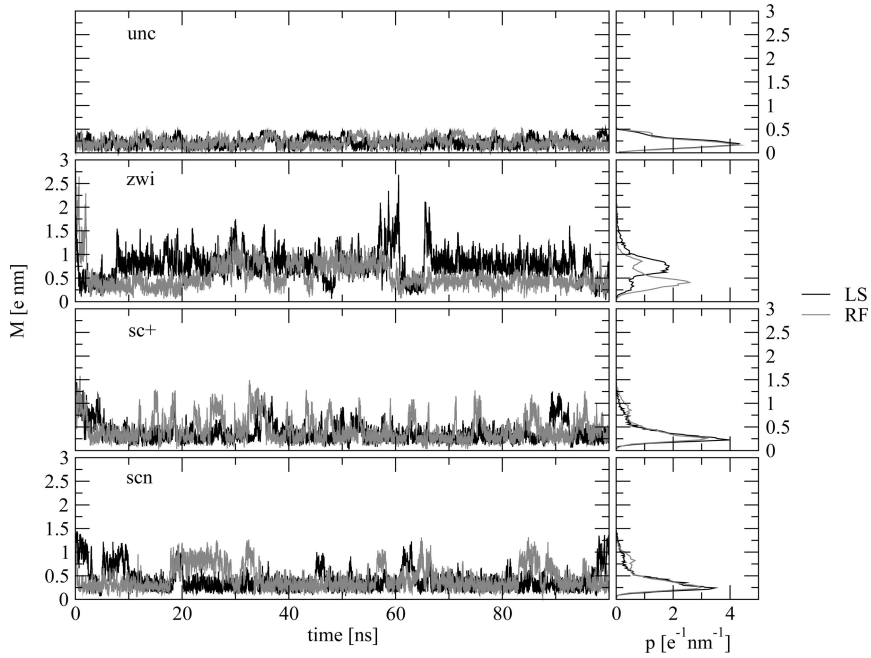

Figure 5. Time evolution and normalized probability distribution (p) of the peptide dipole-moment magnitude M. Simulations using LS and RF electrostatics are shown in black and gray, respectively. From top to bottom (Table 3): uncharged termini (unc); zwitterionic (zwi); singly charged N-terminus, no counterion (sc+); singly charged N-terminus, one neutralizing chloride counterion (scn). For the systems scn and sc+ (peptide with a net charge), the value of M is origin-dependent and is calculated relative to the peptide center of charge.

peptide dipole-moment magnitude ($M \gg 0.5$ e·nm) in the sc+ and scn simulations.

In the zwi simulations (for both LS and RF electrostatics), the time evolutions of M essentially hop on a long time scale between two states, as was the case for the end-to-end distance (Figure 2). The time evolutions of the two latter quantities are actually highly correlated with each other, as well as anticorrelated with the time evolution of the RMSD (Figure 1). The system oscillates between the high-dipole (about 0.8 e·nm) folded helical state and the low-dipole (about 0.3 e·nm) unfolded salt-bridged configurations.

Except for the zwitterionic case, the M distributions are essentially insensitive to the electrostatic scheme employed in the simulation. In the unc case, the distributions present a narrow peak centered at 0.2 e·nm, with a sharp upper bound at 0.5 e·nm. In the sc+ and scn cases, a sharp peak is also found at 0.2 e·nm, but with a borader upper tail extending to 1.4 e·nm. In the zwi case, both LS and RF simulations present the same two high-density regions, but with different populations, as was the case for the RMSD (Figure 1) and D_{EE} (Figure 2). The LS simulation preferentially samples the more polar helical state, whereas the RF simulation predominantly visits the less polar salt-bridged configurations. Note, however, that the configurations with $M > 0.50$ e·nm also encompass about 20−30% unfolded configurations (RMSD > 0.2 nm) in both simulations.

The results of the continuum electrostatics analysis based on trajectory configurations of the zwitterionic peptide (zwi) sampled at 100-ps intervals are presented in Figure 6, where the periodicity-induced perturbation of the electrostatic free energy ($\Delta\Delta G_{el}^{LS}$) associated with a change from nonperiodic Coulombic electrostatics to periodic LS electrostatics is displayed as a function of time for the two simulations (generated using either LS or RF electrostatics). The direct intrasolute (ΔE_{dir}^{LS}) and solvation ($\Delta\Delta G_{slv}^{LS}$) contributions to this quantity (eq 2) are also presented. As observed in previous work,[172,175,251,252] the two contributions are strongly anticorrelated. This is the case because, in the limit of small (nonpolarizable) solute cavities, one expects a relationship of the form of eq 9. The resulting correlation suggested by eq 10 is illustrated in Figure 7. A regression analysis leads to a correlation coefficient of 0.99 and an estimated value of 15.6 for ϵ_S (in excellent agreement with the value of $\epsilon_S = 15$ used for the continuum electrostatics analysis).

Considering the system as a two-state system (Figures 1, 2, and 5), namely, a high-dipole folded helical state and a set of low-dipole unfolded salt-bridged conformations, the following observations can be made. The quantity $\Delta\Delta G_{el}^{LS}$ essentially vanishes in the salt-bridged conformations, whereas it takes an average value of -0.06 kJ·mol^{-1} in the helical state (RMSD < 0.2 nm). Thus, artificial periodicity (solvent-screened interaction

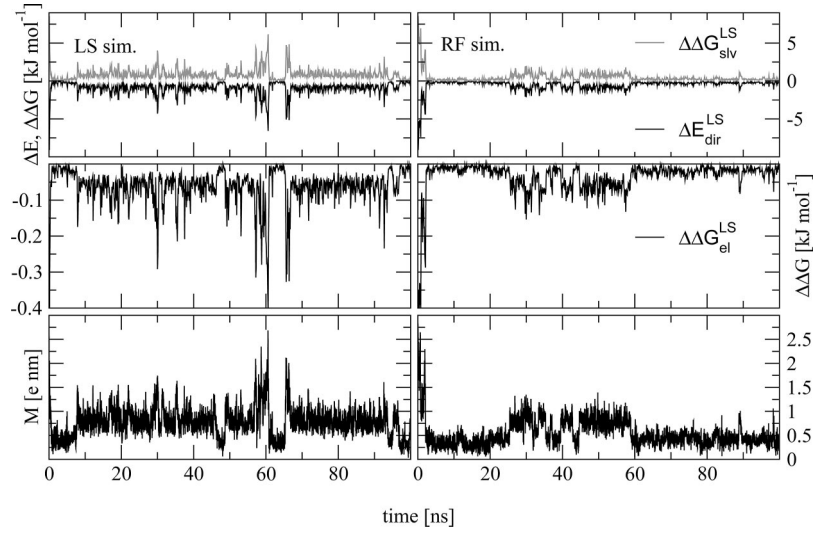

Figure 6. Time evolution of the periodicity-induced perturbation of the electrostatic free energy ($\Delta\Delta G^{LS}_{el}$) associated with a change from nonperiodic Coulombic electrostatics to periodic LS electrostatics, together with the corresponding direct intrasolute (ΔE^{LS}_{dir}) and solvation ($\Delta\Delta G^{LS}_{slv}$) contributions to this quantity (eq 2). Left: frames sampled at 100-ps intervals along the trajectory of the zwitterionic peptide (zwi; Table 1) generated using LS electrostatics. Right: frames sampled at 100-ps intervals along the trajectory of the zwitterionic peptide (zwi; Table 1) generated using RF electrostatics. The time evolution of the peptide dipole-moment magnitude (M; Figure 5) is also shown for comparison.

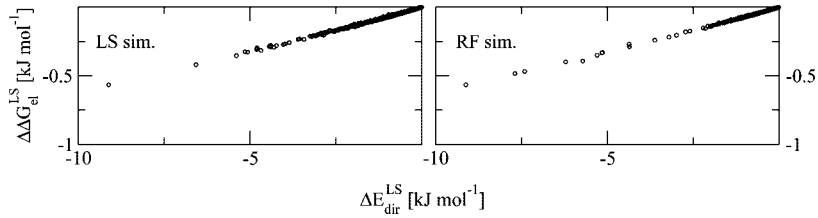

Figure 7. Correlation between the periodicity-induced perturbation of the electrostatic free energy ($\Delta\Delta G^{LS}_{el}$) associated with a change from nonperiodic Coulombic electrostatics to periodic LS electrostatics and the corresponding perturbation of the direct intrasolute interaction (ΔE^{LS}_{dir}) contribution (eq 10). Left: frames sampled at 100-ps intervals along the trajectory of the zwitterionic peptide (zwi; Table 1) generated using LS electrostatics. Right: frames sampled at 100-ps intervals along the trajectory of the zwitterionic peptide (zwi; Table 1) generated using RF electrostatics.

of the peptide dipole in the reference box with its periodic images) stabilizes the high-dipole helical state, in qualitative agreement with previous observations made in the context of a zwitterionic polyalanine octapeptide in water.[252] However, because of the significantly larger box size considered in the present study, this artificial stabilization is more than an order of magnitude smaller here than the thermal energy $k_BT \approx 2.8$ kJ·mol^{-1} at $T = 340$ K, k_B being Boltzmann's constant. Furthermore, the periodicity-induced stabilization never exceeds about -0.4 kJ·mol^{-1} ($-0.14\ k_BT$) even for the most extended structures sampled during the two simulations ($D_{EE} \approx 2.5$ nm). Therefore, the LS scheme represents an accurate way to model electrostatic interactions in the zwi system, given the relatively large box size used in the present simulations (i.e., it appropriately mimics the bulk situation of nonperiodic Coulombic interactions at infinite dilution; this might, however, no longer be the case for smaller box sizes[252]).

The above continuum electrostatics analysis clearly rules out the possibility of a significant bias induced by artificial periodicity in the LS simulation of the zwi system (for the given box size). This conclusion probably also holds for the three other systems (unc, scn, and sc+), where the periodicity-induced perturbation is likely to be of an even smaller magnitude. One is therefore bound to conclude that the differences in the conformational distributions obtained from the explicit-solvent simulations of the zwi and, to a lesser extent, sc+ and scn systems (Figures 1, 2, 4, and 5) using the LS or the RF scheme stem either from insufficient sampling or from a significant bias induced by approximate electrostatics in the RF scheme. The present simulation times (100 ns) are not yet sufficient to guarantee a representative conformational sampling of the considered systems (especially for the LS simulation of the zwi system, where only two folding−unfolding transitions are observed). However, when considered in light of previous simulation and continuum electrostatics studies suggesting deficiencies of the RF scheme in the description of the interaction and pair distributions between solvated species bearing net charges, the differences observed here can almost certainly be attributed to the presence of RF artifacts in the zwi and, to a lesser extent, sc+ and scn systems.

For example, the present observations for the zwi system can be compared to continuum electrostatics analyses made previously in the simpler context of the potential of mean force for the interaction between two spherical ions of opposite charges in water.[175−178] In the LS case, periodicity-induced artifacts were shown to decrease the magnitude of the mean attractive force (including solvents effects) between the two ions over the whole range of interionic distances (see ref 175 and Figures 5a and 6 therein). However, this effect was found to be essentially negligible (in comparison with k_BT) for small spherical ions in reasonably large boxes. The present continuum electrostatics calculations show that these two conclusions also hold for the zwi peptide system (i.e., even for a solvent of lower permittivity and in the presence of the nonpolarizable solute cavity). In the RF case, artifacts due to approximate electrostatics were shown to give rise to a spurious maximum just below and a spurious minimum just above the cutoff distance in the potential of mean force (see ref 177 and Figure 6d therein, as well as ref 178 and

Figure 7c therein). These effects were found to be significant (in comparison with k_BT) even for small spherical ions and might be further enhanced in the present case by the lower permittivity of the solvent and the presence of the solute nonpolarizable cavity. In the zwi system, such a perturbation is expected to induce a decrease in the D_{EE} probability distribution just below 1.4 nm and a corresponding increase just above 1.4 nm. These expectations are in line with the differences in the D_{EE} probability distributions observed between the LS and RF schemes (Figure 2). The RF scheme penalizes configurations with D_{EE} in the upper range for the folded helical state (just below 1.4 nm) at the benefit of the other stable configurations (salt-bridged configurations in the present case). The fact that no additional peak is seen with $D_{EE} > 1.4$ nm does not neccesarily contradict this interpretation, as this absence is probably caused by a low intrinsic stability of these conformations relative to those of the two most populated ones (so that the artificial stabilization by the RF scheme remains insufficient to promote their appearance).

The present observations concerning the performance of the RF scheme in the four different systems (assuming a sufficient level of convergence of the simulations) are also in line with conclusions reached in a number of previous explicit-solvent simulations, which can be summarized as follows (given the typical cutoff distances used in explicit-solvent RF simulations): (i) The RF scheme provides an accurate description of the interaction and pair distributions (radial and orientational) between neutral (dipolar) species (e.g., solvent−solvent in a pure liquid) in polar solvents (far superior to the SC scheme and comparable to the LS scheme).[95,98,99,174,190,207−210,220,225,248,249] (ii) The RF scheme provides a reasonable description of the interaction and pair distributions (radial and orientational) between charged and neutral (dipolar) species (e.g., ion−solvent for a single solvated ion) in polar solvents (far superior to the SC scheme and probably the most accurate among possible MT schemes,[227,230] but affected by small cutoff artifacts).[97,101,104,169,219,250] (iii) The RF scheme provides a poor description of the interaction and pair distributions between charged species (e.g., ion−ion, charged solute functional groups relative to each other or with counterions), even in polar solvents.[101,177,178,202,231,247]

IV. Conclusion

In the present study, eight 100-ns MD simulations of a β-heptapeptide in methanol at 340 K (within cubic computational boxes of about 6-nm edge length) have been reported and compared. The simulations were performed with three different charge-state combinations at the peptide termini, one of them with or without a neutralizing chloride counterion, and using either the LS or the RF scheme to handle electrostatic interactions.

Judging from the monitored properties, the electrostatic scheme appears to have essentially no influence on the folding−unfolding equilibrium when the peptide termini are uncharged. In this case, the peptide remains unfolded with a predominance of rather extended conformations. The influence of the electrostatic scheme is only moderate when the peptide is charged at its N-terminus only (either with or without a neutralizing chloride counterion), except concerning the probability distribution of the distance between the charged N-terminus and the chloride counterion (whenever present). In these simulations, folded and unfolded configurations are present with comparable populations at equilibrium (the unfolded-state ensemble comprising here configurations with a similar extension as the folded state as well as more extended configurations). However, significant differences are observed when both peptide termini are charged (zwitterionic peptide). In this case, the peptide samples predominantly one of the two following states: either a high-dipole helical folded state or a low-dipole salt-bridged unfolded state. The former state prevails in the LS simulation, whereas the latter prevails in the RF simulation.

A continuum electrostatics analysis of the sampled configurations (zwitterionic peptide only) indicates that the artificial periodicity imposed in the LS scheme leads to a marginal stabilization (0.02 k_BT on average) of the helical state but leaves the salt-bridged state essentially unaffected. Such a stabilization can be understood in terms of a favorable (solvent-screened) electrostatic interaction between the termini of the peptide in the reference box and the opposite termini of its periodic copies in the two neighboring boxes along the direction of its end-to-end axis. The very low magnitude of this effect in the present study is most likely due to the use of a large computational box (compared to the size of the nonpolarizable solute cavity) and the relatively high polarity of the solvent.

These results provide clear evidence (continuum electrostatics analysis) for the absence of any significant periodicity-induced artifacts in the LS scheme (for the considered system and box size). As a consequence, the differences observed between the LS and RF schemes in terms of sampled conformations for the zwitterionic (and, to a lesser extent, singly charged) peptide provide some indications for the presence of a significant bias induced by the application of the RF scheme (for the considered system, cutoff distance, and box size). The latter statement is not definitive, because the present simulation times (100 ns) are not yet sufficient to guarantee a representative conformational sampling of the system considered (especially in the LS case). However, the suggestion of major deficiencies of the RF scheme in the description of the interaction and pair distributions between solvated species bearing net charges is in line with previous evidence from continuum electrostatics analyses and explicit-solvent simulations.

The assessment of the relative merits of different approximate electrostatic schemes in explicit-solvent MD simulations is a difficult task because the corresponding errors are (i) difficult to disentangle from other errors caused by incomplete sampling and force-field inaccuracies and (ii) strongly dependent in their nature and magnitude on the type of system considered (in particular, through the presence or absence of ions or charged solute functional groups, the size of the solute nonpolarizable cavity, and the polarity of the solvent) and on the selected simulation parameters (box size, cutoff distance). However, it is also an extremely important task, because electrostatic artifacts can be so large in magnitude that they qualitatively alter the conclusions of a simulation study concerning the investigated system. It is our hope that, in the near future, an increase in computational efficiency (and, thus, in the reachable time scales), the development of methods to artificially accelerate the sampling in MD, and the application of continuum electrostatics analyses will finally permit the formulation of unambiguous conclusions concerning this issue.

Acknowledgment. Financial support from the Swiss National Science Foundation (Project 200020-109261/1) is gratefully acknowledged.

References and Notes

(1) Berendsen, H. J. C. Treatment of long-range forces in molecular dynamics. In *Molecular Dynamics and Protein Structure (Proceedings of a Workshop Held 13−18 May 1984, at University of North Carolina)*; Hermans, J., Ed.; Polycrystal Book Service: Western Springs, IL, 1985; pp 18−22.

(2) Berendsen, H. J. C.; Hol, W. G. J. *Europhys. News* **1986**, *17*, 8.

(3) Harvey, S. C. *Proteins: Struct. Funct. Genet.* **1989**, *5*, 78.

(4) van Gunsteren, W. F.; Berendsen, H. J. C. *Angew. Chem., Int. Ed.* **1990**, *29*, 992.

(5) Davis, M. E.; McCammon, J. A. *Chem. Rev.* **1990**, *90*, 509.

(6) Smith, P. E.; van Gunsteren, W. F. Methods for the evaluation of long range electrostatic forces in computer simulations of molecular systems. In *Computer Simulation of Biomolecular Systems, Theoretical and Experimental Applications*; van Gunsteren, W. F., Weiner, P. K., Wilkinson, A. J., Eds.; ESCOM Science Publishers, B.V.: Leiden, The Netherlands, 1993; Vol. 2, pp 182−212.

(7) Berendsen, H. J. C. Electrostatic interactions. In *Computer Simulation of Biomolecular Systems, Theoretical and Experimental Applications*; van Gunsteren, W. F., Weiner, P. K., Wilkinson, A. J., Eds.; ESCOM Science Publishers, B.V.: Leiden, The Netherlands, 1993; Vol. 2, pp 161−181.

(8) Gilson, M. K. *Curr. Opin. Struct. Biol.* **1995**, *5*, 216.

(9) Brooks, C. L., III. *Curr. Opin. Struct. Biol.* **1995**, *5*, 211.

(10) Levy, R. M.; Gallicchio, E. *Annu. Rev. Phys. Chem.* **1998**, *49*, 531.

(11) Cheatham, T. E., III; Brooks, B. R. *Theor. Chem. Acc.* **1998**, *99*, 279.

(12) Warshel, A.; Papazyan, A. *Curr. Opin. Struct. Biol.* **1998**, *8*, 211.

(13) Darden, T.; Perera, L.; Li, L.; Pedersen, L. *Structure* **1999**, *7*, R55.

(14) Sagui, C.; Darden, T. A. *Annu. Rev. Biophys. Biomol. Struct.* **1999**, *28*, 155.

(15) Hünenberger, P. H.; Börjesson, U.; Lins, R. D. *Chimia* **2001**, *55*, 861.

(16) Hansson, T.; Oostenbrink, C.; van Gunsteren, W. F. *Curr. Opin. Struct. Biol.* **2002**, *12*, 190.

(17) Karplus, M.; McCammon, J. A. *Nat. Struct. Biol.* **2002**, *9*, 646.

(18) Gibbon, P.; Sutmann, G. Long-range interactions in many-particle simulation. In: *Quantum Simulations of Complex Many-Body Systems: From Theory to Algorithms*; Lecture Notes, NIC Series; Grotendorst, J., Marx, D., Muramatsu, A., Eds.; John von Neumann Institute for Computing: Jülich, Germany, 2002; Vol. 10, pp 467−506.

(19) Norberg, J.; Nilsson, L. *Q. Rev. Biophys.* **2003**, *36*, 257.

(20) Koehl, P. *Curr. Opin. Struct. Biol.* **2006**, *16*, 142.

(21) Warshel, A.; Sharma, P. K.; Kato, M.; Parson, W. W. *Biochim. Biophys. Acta* **2006**, *1764*, 1647.

(22) Adcock, S. A.; McCammon, J. A. *Chem. Rev.* **2006**, *106*, 1589.

(23) van Gunsteren, W. F.; Bakowies, D.; Baron, R.; Chandrasekhar, I.; Christen, M.; Daura, X.; Gee, P.; Geerke, D. P.; Glättli, A.; Hünenberger, P. H.; Kastenholz, M. A.; Oostenbrink, C.; Schenk, M.; Trzesniak, D.; van der Vegt, N. F. A.; Yu, H. B. *Angew. Chem., Int. Ed.* **2006**, *45*, 4064.

(24) Monticelli, L.; Colombo, G. *Theor. Chem. Acc.* **2004**, *112*, 145.

(25) Baumketner, A.; Shea, J.-E. *J. Phys. Chem. B* **2005**, *109*, 21322.

(26) Villarreal, M. A.; Montich, G. G. *J. Biomol. Struct. Dyn.* **2005**, *23*, 135.

(27) Monticelli, L.; Simões, C.; Belvisi, L.; Colombo, G. *J. Phys.: Condens. Matter* **2006**, *18*, 329.

(28) Alder, B. J.; Wainwright, T. E. *J. Chem. Phys.* **1959**, *31*, 459.

(29) Allen, M. P.; Tildesley, D. J. *Computer Simulation of Liquids*; Oxford University Press: New York, 1987.

(30) Bekker, H. *J. Comput. Chem.* **1997**, *18*, 1930.

(31) Berkowitz, M.; McCammon, J. A. *Chem. Phys. Lett.* **1982**, *90*, 215.

(32) Brooks, C. L.; Karplus, M. *J. Chem. Phys.* **1983**, *79*, 6312.

(33) Belch, A. C.; Berkowitz, M. *Chem. Phys. Lett.* **1985**, *113*, 278.

(34) Warshel, A.; King, G. *Chem. Phys. Lett.* **1985**, *121*, 124.

(35) King, G.; Warshel, A. *J. Chem. Phys.* **1989**, *91*, 3647.

(36) Juffer, A. H.; Berendsen, H. J. C. *Mol. Phys.* **1993**, *79*, 623.

(37) Beglov, D.; Roux, B. *J. Chem. Phys.* **1994**, *100*, 9050.

(38) Essex, J. W.; Jorgensen, W. L. *J. Comput. Chem.* **1995**, *16*, 951.

(39) Montoro, J. C. G.; Abascal, J. L. F. *Mol. Simul.* **1995**, *14*, 313.

(40) Beglov, D.; Roux, B. *Biopolymers* **1995**, *35*, 171.

(41) Lounnas, V.; Lüdemann, S. K. *Biophys. Chem.* **1999**, *78*, 157.

(42) Im, W.; Berbèche, S.; Roux, B. *J. Chem. Phys.* **2001**, *117*, 2924.

(43) Petraglio, G.; Ceccarelli, M.; Parrinello, M. *J. Chem. Phys.* **2005**, *123*, 044103/1.

(44) Riihimäki, E.-S.; Martínez, J. M.; Kloo, L. *J. Mol. Struct.* **2006**, *760*, 91.

(45) Brancato, G.; Rega, N.; Barone, V. *J. Chem. Phys.* **2006**, *124*, 21405/1.

(46) Li, Y.; Krilov, G.; Berne, B. J. *J. Phys. Chem. B.* **2006**, *110*, 13256.

(47) Ewald, P. P. *Ann. Phys.* **1921**, *64*, 253.

(48) de Leeuw, S. W.; Perram, J. W.; Smith, E. R. *Proc. R. Soc. London A* **1980**, *373*, 27.

(49) de Leeuw, S. W.; Perram, J. W.; Smith, E. R. *Proc. R. Soc. London A* **1980**, *373*, 57.

(50) Luty, B. A.; Davis, M. E.; Tironi, I. G.; van Gunsteren, W. F. *Mol. Simul.* **1994**, *14*, 11.

(51) Darden, T. A.; Toukmaji, A.; Pedersen, L. G. *J. Chim. Phys.* **1997**, *94*, 1346.

(52) Deserno, M.; Holm, C. *J. Chem. Phys.* **1998**, *109*, 7678.

(53) Deserno, M.; Holm, C. *J. Chem. Phys.* **1998**, *109*, 7694.

(54) Hünenberger, P. H. Lattice-sum methods for computing electrostatic interactions in molecular simulations. In *Simulation and Theory of Electrostatic Interactions in Solution: Computational Chemistry, Biophysics, and Aqueous Solution*; Hummer, G., Pratt, L. R., Eds.; American Institute of Physics: New York, 1999; pp 17−83.

(55) Lekner, J. *Physica A* **1989**, *157*, 826.

(56) Lekner, J. *Physica A* **1991**, *176*, 485.

(57) Sperb, R. *Mol. Simul.* **1994**, *13*, 189.

(58) Gronbech-Jensen, N. *Int. J. Mod. Phys. C* **1997**, *8*, 1287.

(59) Mazars, M. *J. Chem. Phys.* **2001**, *115*, 2955.

(60) English, N. J.; Macelroy, J. M. D. *Mol. Phys.* **2002**, *100*, 3753.

(61) Mazars, M. *Mol. Phys.* **2005**, *103*, 1241.

(62) Evjen, H. M. *Phys. Rev.* **1932**, *39*, 675.

(63) Gurney, I. D. C. *Phys. Rev.* **1952**, *90*, 317.

(64) Krishnan, K. S.; Roy, S. K. *Phys. Rev.* **1952**, *87*, 581.

(65) Dahl, J. P. *J. Phys. Chem. Solids* **1965**, *26*, 33.

(66) Hockney, R. W., Eastwood, J. W. *Computer Simulation Using Particles*; McGraw-Hill: New York, 1981.

(67) Darden, T.; York, D.; Pedersen, L. *J. Chem. Phys.* **1993**, *98*, 10089.

(68) Essmann, U.; Perera, L.; Berkowitz, M. L.; Darden, T.; Lee, H.; Pedersen, L. G. *J. Chem. Phys.* **1995**, *103*, 8577.

(69) Greengard, L.; Rokhlin, V. *J. Comput. Phys.* **1987**, *73*, 325.

(70) Schmidt, K. E.; Lee, M. A. *J. Stat. Phys.* **1991**, *63*, 1223.

(71) Ding, H.-Q.; Karasawa, N.; Goddard, W. A., III. *Chem. Phys. Lett.* **1992**, *196*, 6.

(72) Shimada, J.; Kaneko, H.; Takada, T. *J. Comput. Chem.* **1993**, *14*, 867.

(73) Shimada, J.; Kaneko, H.; Takada, T. *J. Comput. Chem.* **1994**, *15*, 28.

(74) Pollock, E. L.; Glosli, J. *Comput. Phys. Commun.* **1996**, *95*, 93.

(75) Lambert, C. G.; Darden, T. A.; Board, J. A., Jr. *J. Comput. Phys.* **1996**, *126*, 274.

(76) Challacombe, M.; White, C.; Head-Gordon, M. *J. Chem. Phys.* **1997**, *107*, 10131.

(77) Figueirido, F.; Levy, R. M.; Zhou, R.; Berne, B. J. *J. Phys. Chem.* **1997**, *106*, 9835.

(78) Schmidt, K. E.; Lee, M. A. *J. Stat. Phys.* **1997**, *89*, 411.

(79) Kudin, K. N.; Scuseria, G. E. *Chem. Phys. Lett.* **1998**, *283*, 61.

(80) Duan, Z.-H.; Krasny, R. *J. Chem. Phys.* **2000**, *113*, 3492.

(81) Kudin, K. N.; Scuseria, G. E. *Phys. Rev. B* **2000**, *61*, 5141.

(82) Zheng, J.; Balasundaram, R.; Gehrke, S. H.; Heffelfinger, G. S.; Goddard, W. A., III; Jiang, S. *J. Chem. Phys.* **2003**, *118*, 5347.

(83) Ogata, S.; Campbell, T. J.; Kalia, R. K.; Nakano, A.; Vashishta, P.; Vemparala, S. *Comput. Phys. Commun.* **2003**, *153*, 445.

(84) Kudin, K. N.; Scuseria, G. E. *J. Chem. Phys.* **2004**, *121*, 2886.

(85) Merrick, M. P.; Iyer, K. A.; Beck, T. L. *J. Phys. Chem.* **1995**, *99*, 12478.

(86) Sagui, C.; Darden, T. *J. Chem. Phys.* **2001**, *114*, 6578.

(87) Izaguirre, J. A.; Hampton, S. S.; Matthey, T. *J. Parallel. Distrib. Comput.* **2005**, *65*, 949.

(88) York, D. M.; Yang, W. *J. Chem. Phys.* **1994**, *101*, 3298.

(89) Genovese, L.; Deutsch, T.; Godecker, T. *J. Chem. Phys.* **2007**, *127*, 054704/1.

(90) Maggs, A. C. *J. Chem. Phys.* **2002**, *117*, 1975.

(91) Maggs, A. C.; Rosetto, V. *Phys. Rev. Lett.* **2002**, *88*, 196402/1.

(92) Rottler, J. *J. Chem. Phys.* **2004**, *120*, 3119.

(93) Rottler, J.; Maggs, A. C. *Phys. Rev. Lett.* **2004**, *93*, 170201/1.

(94) Maggs, A. C. *Comput. Phys. Commun.* **2005**, *169*, 160.

(95) Barker, J. A.; Watts, R. O. *Mol. Phys.* **1973**, *26*, 789.

(96) Barker, J. A. *Mol. Phys.* **1994**, *83*, 1057.

(97) Tironi, I. G.; Sperb, R.; Smith, P. E.; van Gunsteren, W. F. *J. Chem. Phys.* **1995**, *102*, 5451.

(98) Hünenberger, P. H.; van Gunsteren, W. F. *J. Chem. Phys.* **1998**, *108*, 6117.

(99) Mathias, G.; Egwolf, B.; Nonella, M.; Tavan, P. *J. Chem. Phys.* **2003**, *118*, 10847.

(100) Heinz, T. N.; Hünenberger, P. H. *J. Chem. Phys.* **2005**, *123*, 034107/1.

(101) Hummer, G.; Soumpasis, D. M.; Neumann, M. *Mol. Phys.* **1992**, *77*, 769.

(102) Müller-Plathe, F. *Comput. Phys. Commun.* **1993**, *78*, 77.

(103) Kastenholz, M. A.; Hünenberger, P. H. *J. Chem. Phys.* **2006**, *124*, 124106/1.
(104) Kastenholz, M. A.; Hünenberger, P. H. *J. Chem. Phys.* **2006**, *124*, 224501/1.
(105) Brooks, B. R.; Bruccoleri, R. E.; Olafson, B. D.; States, D. J.; Swaminathan, S.; Karplus, M. *J. Comput. Chem.* **1983**, *4*, 187.
(106) Brooks, C. L., III; Pettitt, B. M.; Karplus, M. *J. Chem. Phys.* **1985**, *83*, 5897.
(107) Loncharich, R. J.; Brooks, B. R. *Proteins: Struct. Funct. Genet.* **1989**, *6*, 32.
(108) Stote, R. H.; States, D. J.; Karplus, M. *J. Chim. Phys.* **1991**, *88*, 2419.
(109) Ding, H.-Q.; Karasawa, N.; Goddard, W. A., III. *Chem. Phys. Lett.* **1992**, *193*, 197.
(110) Guenot, J.; Kollman, P. A. *J. Comput. Chem.* **1993**, *14*, 295.
(111) Steinbach, P. J.; Brooks, B. R. *J. Comput. Chem.* **1994**, *15*, 667.
(112) Norberg, J.; Nilsson, L. *Biophys. J.* **2000**, *79*, 1537.
(113) Adams, D. J.; Dubey, G. S. *J. Comput. Phys.* **1987**, *72*, 156.
(114) Kim, K. S. *Chem. Phys. Lett.* **1989**, *156*, 261.
(115) Prevost, M.; van Belle, D.; Lippens, G.; Wodak, S. *Mol. Phys.* **1990**, *71*, 587.
(116) Hummer, G.; Soumpasis, D. M. *Phys. Rev. E* **1994**, *49*, 591.
(117) Hummer, G.; Soumpasis, D. M. *J. Phys.: Condens. Matter* **1994**, *6*, A141.
(118) Hummer, G.; Pratt, L. R.; Garcia, A. E. *J. Phys. Chem.* **1996**, *100*, 1206.
(119) Yakub, E.; Ronchi, C. *J. Chem. Phys.* **2003**, *119*, 11556.
(120) Beck, D. A. C.; Armen, R. S.; Daggett, V. *Biochemistry* **2005**, *44*, 609.
(121) Wu, X.; Brooks, B. R. *J. Chem. Phys.* **2005**, *122*, 044107/1.
(122) Yakub, E.; Ronchi, C. *J. Low Temp. Phys.* **2005**, *139*, 633.
(123) Yakub, E. *J. Phys. A: Math. Gen.* **2006**, *39*, 4643.
(124) Wolf, D.; Keblinski, S. R.; Phillpot, S. R.; Eggebrecht, J. *J. Chem. Phys.* **1999**, *110*, 8254.
(125) Zahn, D.; Schilling, B.; Kast, S. M. *J. Phys. Chem. B* **2002**, *106*, 10725.
(126) Ma, Y.; Garofalini, S. H. *Mol. Simul.* **2005**, *31*, 739.
(127) Fennell, C. J.; Gezelter, J. D. *J. Chem. Phys.* **2006**, *124*, 234104/1.
(128) Tasaki, K.; McDonald, S.; Brady, J. W. *J. Comput. Chem.* **1993**, *14*, 278.
(129) Garemyr, R.; Elofsson, A. *Proteins: Struct. Funct. Genet.* **1999**, *37*, 417.
(130) Brunsteiner, M.; Boresch, S. *J. Chem. Phys.* **2000**, *112*, 6953.
(131) Mark, P.; Nilsson, L. *J. Comput. Chem.* **2002**, *23*, 1211.
(132) Kuwajima, S.; Warshel, A. *J. Chem. Phys.* **1988**, *89*, 3751.
(133) Lee, F. S.; Warshel, A. *J. Chem. Phys.* **1992**, *97*, 3100.
(134) Alper, H.; Levy, R. M. *J. Chem. Phys.* **1993**, *99*, 9847.
(135) Luty, B. A.; van Gunsteren, W. F. *J. Phys. Chem.* **1996**, *100*, 2581.
(136) Kastenholz, M.; Hünenberger, P. H. *J. Chem. Phys.* **2006**, *124*, 124108/1.
(137) Kratky, K. W. *J. Comput. Phys.* **1980**, *37*, 205.
(138) Kratky, K. W.; Schreiner, W. *J. Comput. Phys.* **1982**, *47*, 313.
(139) Schreiner, W.; Kratky, K. W. *Mol. Phys.* **1983**, *50*, 435.
(140) Caillol, J. M.; Levesque, D. *J. Chem. Phys.* **1991**, *94*, 597.
(141) Caillol, J. M. *J. Chem. Phys.* **1992**, *96*, 1455.
(142) Caillol, J. M.; Levesque, D. *J. Chem. Phys.* **1992**, *96*, 1477.
(143) Caillol, J. M. *J. Chem. Phys.* **1993**, *99*, 8953.
(144) Caillol, J. M. *J. Chem. Phys.* **1999**, *111*, 6528.
(145) Hanassab, S.; Vandernoot, T. J. *Mol. Simul.* **2003**, *2*, 527.
(146) Hanassab, S.; Vandernoot, T. J. *Mol. Simul.* **2004**, *30*, 301.
(147) Råsmark, P. J.; Ekholm, T.; Elvingson, C. *J. Chem. Phys.* **2005**, *122*, 184110/1.
(148) Chen, Z.-M.; Çağin, T.; Goddard, W. A., III. *J. Comput. Chem.* **1997**, *18*, 1365.
(149) Ding, H.-Q.; Karasawa, N.; Goddard, W. A., III. *J. Chem. Phys.* **1992**, *97*, 4309.
(150) In't Veld, P. J.; Ismail, A. E.; Grest, G. S. *J. Chem. Phys.* **2007**, *127*, 144711/1.
(151) Ismail, A. E.; Grest, G. S.; Stevens, M. J. *J. Chem. Phys.* **2006**, *125*, 014702/1.
(152) Karasawa, N.; Goddard, W. A., III. *J. Phys. Chem.* **1989**, *93*, 7320.
(153) Ko, G. H.; Fink, W. H. *J. Comput. Chem.* **2002**, *23*, 477.
(154) Lopez-Lemus, J.; Robero-Bastida, M.; Darden, T. A.; Alejandre, J. *Mol. Phys.* **2006**, *104*, 2413.
(155) Monkenbusch, M. *Comput. Phys. Commun.* **1991**, *67*, 343.
(156) Ou-Yang, W.-Z.; Lu, Z.-Y.; Shi, T.-F.; Sun, Z.-Y.; An, L.-J. *J. Chem. Phys.* **2005**, *123*, 234502/1.
(157) Shi, B.; Sinha, S.; Dir, V. K. *J. Chem. Phys.* **2006**, *124*, 204715/1.
(158) Williams, D. E. *Acta Crystallogr. A* **1971**, *27*, 452.
(159) Blokhuis, E. M.; Bedeaux, D.; Holcomb, C. D.; Zollweg, J. A. *Mol. Phys.* **1995**, *85*, 665.
(160) Chapela, G. A.; Saville, G.; Thompson, S. M.; Rowlinson, J. S. *J. Chem. Soc., Faraday Trans.* **1977**, *73*, 1133.
(161) Ghoufi, A.; Goujon, F.; Lachet, V.; Malfreyt, P. *Phys. Rev. E* **2008**, *77*, 031601/1.
(162) Janeček, J. *J. Phys. Chem. B* **2006**, *110*, 6264.
(163) Janeček, J. *J. Phys. Chem. B* **2006**, *110*, 6916.
(164) Lagüe, P.; Pastor, R. W.; Brooks, B. R. *J. Phys. Chem. B* **2004**, *108*, 363.
(165) Shen, V. K.; Mountain, R. D.; Errington, J. R. *J. Phys. Chem. B* **2007**, *111*, 6198.
(166) Shirts, M. R.; Mobley, D. L.; Chodera, J. D.; Pande, V. S. *J. Phys. Chem. B* **2007**, *111*, 13052.
(167) Roberts, J. E.; Schnitker, J. *J. Phys. Chem.* **1995**, *99*, 1322.
(168) Boresch, S.; Steinhauser, O. *Ber. Bunsen-Ges. Phys. Chem.* **1997**, *101*, 1019.
(169) Boresch, S.; Steinhauser, O. *J. Chem. Phys.* **1999**, *111*, 8271.
(170) Boresch, S.; Steinhauser, O. *J. Chem. Phys.* **2001**, *115*, 10780.
(171) Boresch, S.; Steinhauser, O. *J. Chem. Phys.* **2001**, *115*, 10793.
(172) Kastenholz, M.; Hünenberger, P. H. *J. Phys. Chem. B* **2004**, *108*, 774.
(173) Caillol, J.-M. *J. Chem. Phys.* **1994**, *101*, 6080.
(174) Mathias, G.; Tavan, P. *J. Chem. Phys.* **2004**, *120*, 4393.
(175) Hünenberger, P. H.; McCammon, J. A. *J. Chem. Phys.* **1999**, *110*, 1856.
(176) Peter, C.; van Gunsteren, W. F.; Hünenberger, P. H. *J. Chem. Phys.* **2002**, *116*, 7434.
(177) Peter, C.; van Gunsteren, W. F.; Hünenberger, P. H. *J. Chem. Phys.* **2003**, *119*, 12205.
(178) Bergdorf, M.; Peter, C.; Hünenberger, P. H. *J. Chem. Phys.* **2003**, *119*, 9129.
(179) Auffinger, P.; Beveridge, D. L. *Chem. Phys. Lett.* **1995**, *234*, 413.
(180) Kitson, D. H.; Avbelj, F.; Moult, J.; Nguyen, D. T.; Mertz, J. E.; Hadzi, D.; Hagler, A. T. *Proc. Natl. Acad. Sci. U.S.A.* **1993**, *90*, 8920.
(181) Lau, K. F.; Alper, H. E.; Thatcher, T. S.; Stouch, T. E. *J. Phys. Chem.* **1994**, *98*, 8785.
(182) Auffinger, P.; Louise-May, S.; Westhof, E. *J. Am. Chem. Soc.* **1996**, *118*, 1181.
(183) Fraser, L. M.; Foulkes, W. M. C.; Rajagopal, G.; Needs, R. J.; Kenny, S. D.; Williamson, A. J. *Phys. Rev. B* **1996**, *53*, 1814.
(184) Williamson, A. J.; Rajagopal, G.; Needs, R. J.; Fraser, L. M.; Foulkes, W. M. C.; Wang, Y.; Chou, M.-Y. *Phys. Rev. B* **1997**, *55*, R4851.
(185) Kent, P. R. C.; Hood, R. Q.; Williamson, A. J.; Needs, R. J.; Foulkes, W. M. C.; Rajagopal, G. *Phys. Rev. B* **1999**, *59*, 1917.
(186) Fadrná, E.; Hladečková, K.; Koča, J. *J. Biomol. Struct. Dyn.* **2005**, *23*, 151.
(187) Beglov, D. B.; Lipanov, A. A. *J. Biomol. Struct. Dyn.* **1991**, *9*, 205.
(188) Schreiber, H.; Steinhauser, O. *Chem. Phys.* **1992**, *168*, 75.
(189) Schreiber, H.; Steinhauser, O. *Biochemistry* **1992**, *31*, 5856.
(190) Schreiber, H.; Steinhauser, O. *J. Mol. Biol.* **1992**, *228*, 909.
(191) York, D. M.; Darden, T. A.; Pedersen, L. G. *J. Chem. Phys.* **1993**, *99*, 8345.
(192) Cheatham, T. E., III; Miller, J. L.; Fox, T.; Darden, T. A.; Kollman, P. A. *J. Am. Chem. Soc.* **1995**, *117*, 4193.
(193) Niedermeier, C.; Tavan, P. *J. Chem. Phys.* **1994**, *101*, 734.
(194) Louise-May, S.; Auffinger, P.; Westhof, E. *Curr. Opin. Struct. Biol.* **1996**, *6*, 289.
(195) Zuegg, J.; Gready, J. E. *Biochemistry* **1999**, *38*, 13862.
(196) de Souza, O. N.; Ornstein, R. L. *J. Biomol. Struct. Dyn.* **1999**, *16*, 1205.
(197) Higo, J.; Kono, H.; Nakamura, H.; Sarai, A. *Proteins: Struct. Funct. Genet.* **2000**, *40*, 193.
(198) Walser, R.; Hünenberger, P. H.; van Gunsteren, W. F. *Proteins: Struct. Funct. Genet.* **2001**, *44*, 509.
(199) Tieleman, D. P.; Hess, B.; Sansom, M. S. P. *Biophys. J.* **2002**, *83*, 2393.
(200) Anézo, C.; de Vries, A. H.; Höltje, H.-D.; Tieleman, D. P.; Marrink, S.-J. *J. Phys. Chem. B* **2003**, *107*, 9424.
(201) Patra, M.; Karttunen, M.; Hyvönen, M. T.; Falck, E.; Lindqvist, P.; Vattulainen, I. *Biophys. J.* **2003**, *84*, 3636.
(202) Patra, M.; Karttunen, M.; Hyvönen, M. T.; Falck, E.; Vattulainen, I. *J. Phys. Chem. B* **2004**, *108*, 4485.
(203) Lins, R. D.; Röthlisberger, U. *J. Chem. Theory Comput.* **2006**, *2*, 246.
(204) Cordomí, A.; Edholm, O.; Perez, J. *J. Comput. Chem.* **2007**, *28*, 1017.
(205) Ladd, A. J. C. *Mol. Phys.* **1978**, *36*, 463.
(206) Adams, D. J. *Chem. Phys. Lett.* **1979**, *62*, 329.
(207) Neumann, M.; Steinhauser, O. *Mol. Phys.* **1980**, *39*, 437.
(208) Alper, H.; Levy, R. M. *J. Chem. Phys.* **1989**, *91*, 1242.
(209) Steinhauser, O. *Mol. Phys.* **1982**, *45*, 335.
(210) Neumann, M. *Mol. Phys.* **1983**, *50*, 841.
(211) Brooks, C. L., III. *J. Phys. Chem.* **1986**, *90*, 6680.

(212) Linse, P.; Andersen, H. C. *J. Chem. Phys.* **1986**, *85*, 3027.
(213) Brooks, C. L. *J. Chem. Phys.* **1987**, *86*, 5156.
(214) Madura, J. D.; Pettitt, B. M. *Chem. Phys. Lett.* **1988**, *150*, 105.
(215) Straatsma, T. P.; Berendsen, H. J. C. *J. Chem. Phys.* **1988**, *89*, 5876.
(216) Sloth, P.; Sørensen, T. S. *Chem. Phys. Lett.* **1990**, *173*, 51.
(217) Bader, J. S.; Chandler, D. *J. Phys. Chem.* **1992**, *96*, 6423.
(218) Chipot, C.; Millot, C.; Maigret, B.; Kollman, P. A. *J. Chem. Phys.* **1994**, *101*, 7953.
(219) Perera, L.; Essmann, U.; Berkowitz, M. L. *J. Chem. Phys.* **1994**, *102*, 450.
(220) Smith, P. E.; van Gunsteren, W. F. *Mol. Simul.* **1995**, *15*, 233.
(221) Gabdoulline, R. R.; Zheng, C. *J. Comput. Chem.* **1995**, *16*, 1428.
(222) Del Buono, G. S.; Figueirido, F. E.; Levy, R. M. *Chem. Phys. Lett.* **1996**, *263*, 521.
(223) Kalko, S. G.; Sese, G.; Padro, J. A. *J. Chem. Phys.* **1996**, *104*, 9578.
(224) Resat, H.; McCammon, J. A. *J. Chem. Phys.* **1996**, *104*, 7645.
(225) Tironi, I. G.; Luty, B. A.; van Gunsteren, W. F. *J. Chem. Phys.* **1997**, *106*, 6068.
(226) Resat, H.; McCammon, J. A. *J. Chem. Phys.* **1998**, *108*, 9617.
(227) Baker, N. A.; Hünenberger, P. H.; McCammon, J. A. *J. Chem. Phys.* **1999**, *110*, 10679.
(228) Resat, H. *J. Chem. Phys.* **1999**, *110*, 6887.
(229) Nymand, T. M.; Linse, P. *J. Chem. Phys.* **2000**, *112*, 6386.
(230) Baker, N. A.; Hünenberger, P. H.; McCammon, J. A. *J. Chem. Phys.* **2000**, *113*, 2510.
(231) Rozanska, X.; Chipot, C. *J. Chem. Phys.* **2000**, *112*, 9691.
(232) Ledauphin, V.; Vergoten, G. *Biopolymers* **2001**, *57*, 373.
(233) Shinto, H.; Morisada, S.; Miyahara, M.; Higashitani, K. *J. Chem. Eng. Jpn.* **2003**, *36*, 57.
(234) Yonetani, Y. *Chem. Phys. Lett.* **2005**, *406*, 49.
(235) Yonetani, Y. *J. Chem. Phys.* **2006**, *124*, 204501/1.
(236) van der Spoel, D.; van Maaren, P. J. *J. Chem. Theory Comput.* **2006**, *2*, 1.
(237) Król, M. *J. Mol. Model.* **2003**, *9*, 316.
(238) Avbelj, F.; Moult, J.; Kitson, D. H.; James, M. N. G.; Hagler, A. T. *Biochemistry* **1990**, *29*, 8658.
(239) Smith, P. E.; Pettitt, B. M. *J. Chem. Phys.* **1991**, *95*, 8430.
(240) Eichinger, M.; Grubmüller, H.; Heller, H.; Tavan, P. *J. Comput. Chem.* **1997**, *18*, 1729.
(241) Klauda, J. B.; Brooks, B. R.; Pastor, R. W. *J. Chem. Phys.* **2006**, *125*, 144710/1.
(242) Stocker, U.; van Gunsteren, W. F. *Proteins: Struct. Funct. Genet.* **2000**, *40*, 145.
(243) Nina, M.; Simonson, T. *J. Phys. Chem. B* **2002**, *106*, 3696.
(244) Gargallo, R.; Hünenberger, P. H.; Avilés, F. X.; Oliva, B. *Protein Sci.* **2003**, *12*, 2161.
(245) de Vries, A. H.; Chandrasekhar, I.; van Gunsteren, W. F.; Hünenberger, P. H. *J. Phys. Chem. B* **2005**, *109*, 11643.
(246) Walser, R.; Hünenberger, P. H.; van Gunsteren, W. F. *Proteins: Struct. Funct. Genet.* **2002**, *48*, 327.
(247) Kräutler, V.; Hünenberger, P. H. *Mol. Simul.* **2008**, *34*, 491.
(248) Neumann, M.; Steinhauser, O.; Pawley, G. S. *Mol. Phys.* **1984**, *52*, 97.
(249) Belhadj, M.; Alper, H. *Chem. Phys. Lett.* **1991**, *179*, 13.
(250) Reif, M. M.; Hünenberger, P. H., manuscript in preparation.
(251) Hünenberger, P. H.; McCammon, J. A. *Biophys. Chem.* **1999**, *78*, 69.
(252) Weber, W.; Hünenberger, P. H.; McCammon, J. A. *J. Phys. Chem. B* **2000**, *104*, 3668.
(253) Takaoka, Y.; Pasenkievicz-Gierula, M.; Miyagawa, H.; Kitamura, K.; Tamura, Y.; Kusumi, A. *Biophys. J.* **2000**, *79*, 3118.
(254) Wood, R. H. *J. Chem. Phys.* **1995**, *103*, 6177.
(255) Davis, M. E.; McCammon, J. A. *J. Comput. Chem.* **1991**, *12*, 909.
(256) Honig, B.; Sharp, K.; Yang, A.-S. *J. Phys. Chem.* **1993**, *97*, 1101.
(257) Rick, S. W.; Berne, B. J. *J. Am. Chem. Soc.* **1994**, *116*, 3949.
(258) Nina, M.; Beglov, D.; Roux, B. *J. Phys. Chem. B* **1997**, *101*, 5239.
(259) Bruccoleri, R. B.; Novotny, J.; Davis, M. E. *J. Comput. Chem.* **1997**, *18*, 268.
(260) Lee, M. S.; Olson, M. A. *J. Phys. Chem. B* **2005**, *109*, 5223.
(261) Baker, N. A. *Curr. Opin. Struct. Biol.* **2005**, *15*, 137.
(262) Grochowski, P.; Trylska, J. *Biopolymers* **2007**, *89*, 93.
(263) Daura, X.; van Gunsteren, W. F.; Rigo, D.; Jaun, B.; Seebach, D. *Chem. Eur. J.* **1997**, *3*, 1410.
(264) Daura, X.; Gademann, K.; Jaun, B.; Seebach, D.; van Gunsteren, W. F.; Mark, A. E. *Angew. Chem., Intl. Ed.* **1999**, *38*, 236.
(265) Seebach, D.; Abele, S.; Gademann, K.; Guichard, G.; Hintermann, T.; Jaun, B.; Matthews, J. L.; Schreiber, J. V. *Helv. Chim. Acta* **1998**, *81*, 932.
(266) van Gunsteren, W. F.; Billeter, S. R.; Eising, A. A.; Hünenberger, P. H.; Krüger, P.; Mark, A. E.; Scott, W. R. P.; Tironi, I. G. *Biomolecular Simulation: The GROMOS96 Manual and User Guide*; Verlag der Fachvereine: Zürich, Switzerland, 1996.
(267) Scott, W. R. P.; Hünenberger, P. H.; Tironi, I. G.; Mark, A. E.; Billeter, S. R.; Fennen, J.; Torda, A. E.; Huber, T.; Krüger, P.; van Gunsteren, W. F. *J. Phys. Chem. A* **1999**, *103*, 3596.
(268) Schuler, L. D.; Daura, X.; van Gunsteren, W. F. *J. Comput. Chem.* **2001**, *22*, 1205.
(269) Walser, R.; Mark, A. E.; van Gunsteren, W. F.; Lauterbach, M.; Wipff, G. *J. Chem. Phys.* **2000**, *112*, 10450.
(270) Hockney, R. W. *Methods Comput. Phys.* **1970**, *9*, 136.
(271) Ryckaert, J.-P.; Ciccotti, G.; Berendsen, H. J. C. *J. Comput. Phys.* **1977**, *23*, 327.
(272) Berendsen, H. J. C.; Postma, J. P. M.; van Gunsteren, W. F.; Di Nola, A.; Haak, J. R. *J. Chem. Phys.* **1984**, *81*, 3684.
(273) Berendsen, H. J. C.; van Gunsteren, W. F.; Zwinderman, H. R. J.; Geurtsen, R. G. *Ann. N.Y. Acad. Sci.* **1986**, *482*, 269.
(274) Hünenberger, P. H. *J. Chem. Phys.* **2000**, *113*, 10464.
(275) Lide, D. R., Ed. *CRC Handbook of Chemistry and Physics*, 83rd ed.; CRC Press: Boca Raton, FL, 2002.
(276) Parsons, G. H.; Rochester, C. H. *J. Chem. Soc., Faraday Trans. 1* **1972**, *68*, 523.
(277) Rived, F.; Rosés, M.; Bosch, E. *Anal. Chim. Acta* **1998**, *374*, 309.
(278) Redlack, A.; Grindlay, J. *Can. J. Phys* **1972**, *50*, 2815.
(279) Nijboer, B. R. A.; Ruijgrok, T. W. *J. Stat. Phys.* **1988**, *53*, 361.
(280) Cichocki, B.; Felderhof, B. U.; Hinsen, K. *Phys. Rev. A* **1989**, *39*, 5350.
(281) Davis, M. E.; Madura, J. D.; Luty, B. A.; McCammon, J. A. *Comput. Phys. Commun.* **1991**, *62*, 187.
(282) Madura, J. D.; Briggs, J. M.; Wade, R. C.; Davis, M. E.; Luty, B. A.; Ilin, A.; Antosiewicz, J.; Gilson, M. K.; Bagheri, B.; Scott, L. R.; McCammon, J. A. *Comput. Phys. Commun.* **1995**, *91*, 57.
(283) Heinz, T. N.; van Gunsteren, W. F.; Hünenberger, P. H. *J. Chem. Phys.* **2001**, *115*, 1125.
(284) Berendsen, H. J. C.; Postma, J. P. M.; van Gunsteren, W. F.; Hermans, J. Interaction models for water in relation to protein hydration. In *Intermolecular Forces*; Pullman, B., Ed.; Reidel: Dordrecht, The Netherlands, 1981; pp 331−342.
(285) Ferrara, P.; Caflisch, A. *Proc. Natl. Acad. Sci. U.S.A.* **2000**, *97*, 10780.
(286) Kräutler, V.; Kastenholz, M. A.; Hünenberger, P. H. The esra molecular mechanics analysis package; 2005; available at http://sourceforge.net/projects/esra, accessed May 2008. Software publisher: Kräutler, V., Kaskholz, M. A., Hünenberger, P. H.: ETH Zürich, Switzerland.
(287) DeLano, W. L. The PyMOL molecular graphics system; 2002; available at http://www.pymol.org, accessed August 2007. Software publisher: DeLano Scientific: Palo Alto, CA, USA.
(288) Martinek, T. A.; Fueloep, F. *Eur. J. Biochem.* **2003**, *270*, 3657.
(289) Gee, P. J.; van Gunsteren, W. F. *Proteins* **2006**, *63*, 136.
(290) Schreiner, W. *Phys. Rev. B* **1983**, *27*, 3848.
(291) Spohr, E. *J. Chem. Phys.* **1997**, *107*, 6342.
(292) Arbuckle, B. W.; Clancy, P. *J. Chem. Phys.* **2002**, *116*, 5090.
(293) Kast, S. M.; Schmidt, K. F.; Schilling, B. *Chem. Phys. Lett.* **2003**, *367*, 398.
(294) Yeh, I.-C.; Hummer, G. *J. Phys. Chem. B* **2004**, *108*, 15873.
(295) English, N. J. *Mol. Phys.* **2005**, *103*, 1945.
(296) English, N. J. *Mol. Phys.* **2006**, *2*, 243.
(297) Åqvist, J. *J. Phys. Chem.* **1990**, *94*, 8021.
(298) Del Buono, G. S.; Cohen, T. S.; Rossky, P. J. *J. Mol. Liq.* **1994**, *60*, 221.
(299) Roberts, J. E.; Schnitker, J. *J. Chem. Phys.* **1994**, *101*, 5024.
(300) Figueirido, F.; Del Buono, G. S.; Levy, R. M. *J. Phys. Chem. B* **1997**, *101*, 5622.
(301) Hummer, G.; Pratt, L. R.; Garcia, A. E. *J. Phys. Chem. A* **1998**, *102*, 7885.
(302) Bogusz, S.; Cheatham, T. E.; Brooks, B. R. *J. Chem. Phys.* **1998**, *108*, 7070.
(303) Hummer, G.; Pratt, L. R.; Garcia, A. E.; Berne, B. J.; Rick, S. W. *J. Phys. Chem. B* **1997**, *101*, 3017.
(304) Ashbaugh, H. S.; Wood, R. H. *J. Phys. Chem. B* **1998**, *102*, 3844.
(305) Hummer, G.; Pratt, L. R.; Garcia, A. E.; Garde, S.; Berne, B. J.; Rick, S. W. *J. Phys. Chem. B* **1998**, *102*, 3841.
(306) Hummer, G.; Pratt, L. R.; Garcia, A. E. *J. Chem. Phys.* **1997**, *107*, 9275.
(307) Ashbaugh, H. S.; Wood, R. H. *J. Chem. Phys.* **1997**, *106*, 8135.
(308) Darden, T.; Pearlman, D.; Pedersen, L. G. *J. Chem. Phys.* **1998**, *109*, 10921.
(309) Garde, S.; Hummer, G.; Paulaitis, M. E. *J. Chem. Phys.* **1998**, *108*, 1552.
(310) Sakane, S.; Ashbaugh, H. S.; Wood, R. H. *J. Phys. Chem. B* **1998**, *102*, 5673.
(311) Sham, Y. Y.; Warshel, A. *J. Chem. Phys.* **1998**, *109*, 7940.
(312) Åqvist, J.; Hansson, T. *J. Phys. Chem. B* **1998**, *102*, 3837.
(313) Babu, C. S.; Yang, P.-K.; Lim, C. *J. Biol. Phys.* **2002**, *28*, 95.

(314) Vorobjev, Y. N.; Hermans, J. *J. Phys. Chem. B* **1999**, *103*, 10234.
(315) Herce, D. H.; Darden, T.; Sagui, C. *J. Chem. Phys.* **2003**, *119*, 7621.
(316) Warren, G. L.; Patel, S. *J. Chem. Phys.* **2007**, *127*, 064509/1.
(317) Todorova, T.; Hünenberger, P. H.; Hutter, J. *J. Chem. Theor. Comput.* **2008**, *4*, 779.
(318) Figueirido, F.; Del Buono, G. S.; Levy, R. M. *J. Chem. Phys.* **1995**, *103*, 6133.
(319) Lantelme, F.; Turq, P.; Quentrec, B.; Lewis, J. W. E. *Mol. Phys.* **1974**, *28*, 1537.
(320) Smith, P. E.; Dang, L. X.; Pettit, B. M. *J. Am. Chem. Soc.* **1991**, *113*, 67.
(321) Ibragimova, G. T.; Wade, R. C. *Biophys. J.* **1998**, *74*, 2906.
(322) Ibragimova, G. T.; Wade, R. C. *Biophys. J.* **1999**, *77*, 2191.
(323) Smith, P. E.; Blatt, H. D.; Pettitt, B. M. *J. Phys. Chem. B* **1997**, *101*, 3886.
(324) York, D. M.; Wlodawer, A.; Pedersen, L. G.; Darden, T. A. *Proc. Natl. Acad. Sci. U.S.A.* **1994**, *91*, 8715.
(325) Fox, T.; Kollman, P. A. *Proteins: Struct. Funct. Genet.* **1996**, *25*, 315.
(326) Perera, L.; Li, L.; Darden, T.; Monroe, D. M.; Pedersen, L. G. *Biophys. J.* **1997**, *73*, 1847.
(327) Smith, P. E.; Pettitt, B. M. *J. Chem. Phys.* **1996**, *105*, 4289.
(328) Pfeiffer, S.; Fushman, D.; Cowburn, D. *Proteins: Struct. Funct. Genet.* **1999**, *35*, 206.
(329) Baştuğ, T.; Patra, S. M.; Kuyucak, *Chem. Phys. Lett.* **2006**, *425*, 320.
(330) de Souza, O. N.; Ornstein, R. L. *Biophys. J.* **1997**, *72*, 2395.
(331) Mazur, A. K. *J. Am. Chem. Soc.* **2002**, *124*, 14707.
(332) Herce, D. H.; Garcia, A. E. *J. Chem. Phys.* **2006**, *125*, 224711/1.

JP807421A